Abstract

JIANG, LIQIU. The Simulation and Approximation of the First Passage Time of the Ornstein–Uhlenbeck Process of Neuron. (Under the direction of Charles Eugene Smith.)

Neurons communicate with each other via sequences of action potentials. The purpose of this study is to approximate the interval between action potentials which is also called the First Passage Time (FPT), the first time the membrane voltage passes a threshold. The subthreshold depolarization of a neuron receiving a multitude of random synaptic inputs has often been modelled as the Ornstein–Uhlenbeck (OU) process. This model provides an analytically tractable formalism of neuronal membrane voltage mean and variance in terms of a neuron's membrane time constant and the mean of input voltage. Some authors obtained an approximate mean and variance of the FPT for Stein's model with a constant threshold for firing by using Stein's method. They approximated the mean and variance of FPT by using the first term of the Taylor's series expansion. We expect this procedure works for the OU process, a diffusion process. This study finds that Stein's method works

well for the OU process with the small Wiener process parameter. After adding a few other terms of the Taylor's series, the parameter range in which the approximation works well are almost the same as the range in which the first term does. The relationship between the approximation results and the confidence band of the mean and variance of the simulated FPT gives evidence that their parameter range is the same; but, the approximation by two terms of the Taylor's series gives less approximation error. The goodness–of–fit–test shows that the lognormal distribution is close to the distribution of FPT for all the Wiener parameters we used. We compared a lognormal distribution of the FPT, estimated from simulation of the OU process, with the probability density function (pdf) of the FPT, approximated from a transformation of the marginal distribution of membrane voltage at the time at which the mean of membrane voltage passes the threshold. We found that the approximation pdf and the lognormal pdf are almost equally close to the true and unknown pdf when the parameter of the Wiener process is small.

THE SIMULATION AND APPROXIMATION OF THE FIRST PASSAGE TIME OF THE ORNSTEIN-UHLENBECK PROCESS OF NEURON

By

Liqiu Jiang

A thesis submitted to the Graduate Faculty of
North Carolina State University
in partial fulfillment of the
requirements for the Degree of
Master of Science

BIOMATHEMATICS GRADUATE PROGRAM
DEPARTMENT OF STATISTICS

Raleigh

2002

APPROVED BY

_____
Dr. Charles E. Smith

_____ _____
Dr. Marcia L. Gumpertz Dr. Timothy C. Elston

This thesis is dedicated to my parents, Wenxiang Jiang and Junqing Wang, and my husband, Yu Zheng, for everything they've done for me.

BIOGRAPHY

Liqiu Jiang was born September 26, 1974 in Jilin Province, People Republic of China. She received her elementary and secondary education in Jilin province, P. R. China and graduated from Meheikou Fifth High School in 1992.

She received Bachelor of Science degree in Stomatology in Peking University, Health Science Center in July, 1997. In July 2000, she received a Masters of Science degree in Anatomy, Histology and Embryology in the same school. In August 2000, she began working on her Masters of Science degree in Biomathematics with a minor in Statistics at North Carolina State University.

ACKNOWLEDGEMENT

Sincere gratitude is extended to Dr. Charles E. Smith, who provided the author with guidance, encouragement, support, and most importantly an education of the scientific process. Appreciation is also expressed to the other members of the advisory committee, Dr. Timothy C. Elston for his encouragement and support and Dr. Marcia L. Gumpertz for her guidance and instruction in some statistical problems. Finally, the author would like to acknowledge the personal support and encouragement provided by my parents Wenxiang Jiang and Junqing Wang, and my husband, Yu Zheng.

Contents

List of Tables

List of Figures

Chapter 1

Introduction

The first passage time is the theoretical counterpart of the interspike intervals. This follows the generally accepted hypothesis that the information transferred within the nervous system is usually encoded by the timing of spikes (action potential). Therefore, the reciprocal relationship between the frequency on one hand and the interspike interval on the other leads to the study of the distribution of the first passage time. When the distribution is too difficult to obtain, the analysis is usually restricted to its moments, primarily the mean and variance.

The Ornstein–Uhlenbeck process and Stein's model of neuron spike are both examples of the leaky integrate–and–fire (LIF) model. In the LIF model,

the membrane depolarizaion is described as a deterministic leaky integrator. Interspike intervals are identified as periods between a reset of the depolarization after firing (an action potential or a spike) and the consecutive crossing of a fixed firing threshold. This leaky integrate–and–fire model is one of the most common on both application of artificial neural network and description of biological systems and has been studied in [37], [24], [36], [23],[9] and [30].

The OU process has the following properties: the voltage difference between the membrane potential and resting potential at the trigger zone of the neuron is described by a one–dimensional stochastic process $X = \{X(t) : t \geq 0\}$ given by the stochastic differential equation

$$dX(t) = \mu(X(t), t)dt + \sigma(X(t), t)dW(t), \quad X(0) = x_0 \tag{1.1}$$

where $W = \{W(t) : t \geq 0\}$ is a standard Wiener process and μ and σ are real-valued functions, so their arguments satisfy certain regularity conditions [19]. In particular for the OU process, $\sigma(x(t), t) = \sigma > 0$ and $\mu(x(t), t) = -x(t)/\tau + \mu$ where $\tau > 0$ is the membrane constant. Here, the process X represents changes in the membrane potential between two

consecutive neuronal firings (spikes). The reference level for the membrane potential is usually taken to be the resting potential. Some studies examined the effect of random initial values in a leaky integrator with deterministic trajectory. They found that different distributions for the initial value lead to commonly observed interspike interval distributions [18], [21], and [20]. This is why initial voltage (the reset value following a spike) is often assumed to be equal to the resting potential, $x_0 = 0$, i. e., there is no initial afterhyperpolarization. The OU process is appropriate for neurons with a high number of synaptic inputs where each of them has only a slight effect on the cell excitability [27].

Mathematical analysis of the model (see 17) presented by Stein, including its modifications and generalizations, is one of the most common approaches to the theoretical study of neuronal activity. The generally adopted procedure considers the OU process, as a result of diffusion approximation, with the first two infinitesimal moments equal to limiting values of those corresponding to a sequence of Stein's model. The aim of this article is to use the original and modified Stein's approximation method to approximate the FPT of neurons whose activity follows the OU process. In this way the article represents a continuation of the previous work on this topic.

The OU process has been simulated in this article in Section 3.1 in page 25. This study used the approximation method for Stein's model in the OU process, which uses the first term of the Taylor's series. It works well for the OU process with a small Wiener process parameter. After adding more terms of the the Taylor's series, the parameter range for a good approximation is very close to that of the first term. But, the approximation by two terms gives less approximation error. The goodness–of–fit–tests show that the lognormal probability density function fit the FPT very well for all the Wiener process parameters we used. We compared the approximated pdf of FPT derived by Stein's method with lognormal pdf fitted for simulated FPT and found that they are almost equally close to the true and unknown pdf for the small Wiener process parameter.

Chapter 2

Literature Review

2.1 The Biological Background

The generic neuron expresses three anatomical features: dendrites—the portions of the neuron that receive inputs, the soma—the central portion that contains the cell's nucleus and may also receive inputs, and the axon—a tendril that branches and serves as the input to other neurons. Inputs bring signals to the neuron, resulting in a complex symphony of ionic and transmembrane potential changes that can make the soma's excitable membrane produce the crescendo of an action potential [13]. Ignoring much detail, the action potential, a pulse–like depolarization of the neuron's transmembrane

potential, occurs when the potential exceeds a critical threshold and ionic concentrations achieve supercritical values.

The biophysical properties of the membrane have important effects on the action potential generation and conduction. For example, the passive resistive electrical properties of the post synaptic cell affect the time course of the postsynaptic cell potentials generated in it by other cells. The passive electrical properties of the postsynaptic cell also determine how efficiently synaptic potentials are propagated within a cell from their sites of origin to the trigger zone. These features of neuronal functioning contribute to synaptic integration, the process by which a nerve cell adds up all incoming signals and determines whether or not it will generate an action potential. Once an action potential is generated, the speed with which it is conducted from the trigger zone to the axon terminal also depends on the passive electrical properties of axon.

A better way to understand the passive membrane properties is to consider the equivalent circuit of the neuron membrane. The membrane can be thought as a resistor and a a conductor connected in parallel. The nerve cell actually does have conductive, capacitive, and electromotive force components that can be specifically attributed to ion channel proteins, embedded

the lipid bilayer, and the ionic concentration gradient (Na^+, Cl^-, K^+). Although they are biological, the three electrical properties of the membrane are functionally indistinguishable from those of a man-made electronic circuit.

2.2 The Physical Basis for the LIF Model

Figure 2.1 is a complete equivalent circuit of the passive electrical properties of the membrane, with membrane capacitance included. Figure 2.2 is the simplified electrical equivalent circuit that can be used to examine the effects of membrane capacitance on the response of a neuron to injected current. The cell membrane is represented by a capacitor (C) in parallel with a resistor (R), which represents the R_{Na}, R_{Cl}, and R_K element in Figure 2.1. The membrane batteries representing the electromotive forces generated by ion diffusion determine the resting or equilibrium voltage when there are no applied currents. It can be ignored because batteries affect only the absolute value of membrane voltage, not voltage rate of change.

From the circuit in Figure 2.2, we can see that the total membrane current (I_m) is the sum of the ionic current (I_i) and the capacitive current (I_c):

$$I_m = I_i + I_c \tag{2.1}$$

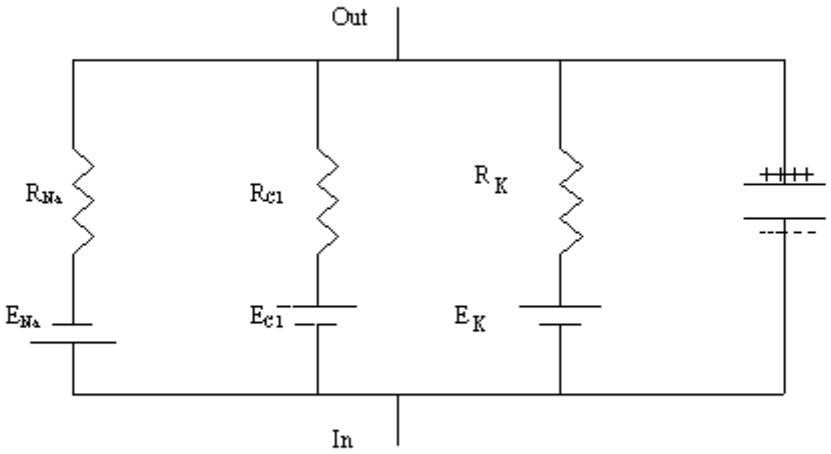

Figure 2.1. The equivalent circuit of cell membrane with three ions.

I_i:Ionic (or resistive) membrane current represents the actual movement of ions through the ion (conductance) channels of the membrane. I_c : Capacitive membrane current represents a change in the net charge stored on the membrane capacitance. Recall that the voltage (V) across a capacitor is

proportional to the charge (Q) stored on the capacitor:

$$V = \frac{Q}{C} \tag{2.2}$$

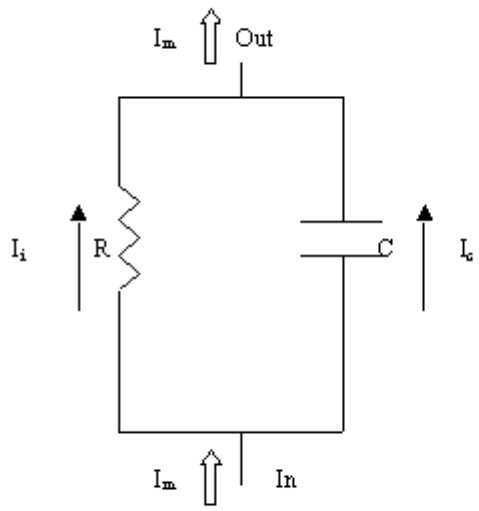

Figure 2.2. The equivalent circuit of cell membrane.

So, for a change in voltage

$$\Delta V_m = \Delta \frac{Q}{C} \tag{2.3}$$

This ΔQ is brought about by the flow of capacitive current (I_c). Also, current is defined as the net movement of positive charge per unit time. The value of capacitive current is equal to the rate at which charge stored on the capacitor changes:

$$I_c = \frac{dQ}{dt} \tag{2.4}$$

Obviously, we can obtain ΔQ by integrating I_c over time.

$$\Delta Q = \int_{t_1}^{t_2} I_c dt \tag{2.5}$$

By substituting to Equation (2.3), we obtain $\Delta V_m \approx \int_{t_1}^{t_2} \frac{I_c \mathrm{d}t}{C}$.

The time course of V_m is slowed by the membrane capacitance. When the V_m is changed by the current injected into the cell, ΔV_m lags behind the current pulse. The reason is that the membrane capacitor and resistor are in parallel; therefore, the potential across these two elements must be equal at all times. The potential across a capacitor can not change until the charge stored on its plates has changed. Initially, all of the membrane current flows

into the capacitor to change the charge on its plates. However, as the pulse continues and ΔQ increases, more and more current must flow through the resistance, because at any instant the voltage drops across the membrane resistor

$$\Delta V_m = I_m R \tag{2.6}$$

must be equal to the voltage across the capacitor

$$\Delta V_m = \frac{\Delta Q}{C}. \tag{2.7}$$

As a larger fraction of the membrane current flows through the resistor, less is available for charging the capacitor; thus the rate of change of V_m decreases with time. When ΔV_m reaches its plateau value, all of the membrane current is flowing through the resistor and

$$V_m = I_m R \tag{2.8}$$

At the end of the current pulse, current flows around the RC loop, as the

capacitor discharges and drives current through resistor. So, we can describe the potential change by the following equation (a usual exponential charging relationship [39]):

$$\Delta V_m(t) = I_m R(1 - e^{-\frac{t}{\tau}}), \tag{2.9}$$

Where τ equals RC, the product of the resistance and capacitance of membrane. The parameter τ is called the membrane time constant.

2.3 The Models

2.3.1 The Ornstein–Uhlenbeck Model

The most common diffusion model is the OU process, which is one substantial step closer to reality than other models, since the spontaneous changes of the membrane potential are included in the model [25].

In Equation 2.9, the steady current source, I, uniformly depolarizes the membrane, causing an exponential increase in its voltage, V. When the membrane voltage reaches a threshold, S, a spike occurs. At this point we shall assume the spike to take an infinitesimal amount of time. We did this because

an action potential is considered to have infinitesimally small duration, the period of each action potential is just the time between interspike intervals. At the spike onset, the membrane capacitor discharges instantaneously, and the membrane potential is reset to the resting potential. This firing process repeats itself as long as the input current is on. The output of a neuron is the sequence of firing. This model is a classic leaky integrate–and–fire model. If we let μ be the input current, then $\mu = \frac{I}{C}$, when the input is on. So, we can rewrite Equation 2.9 as:

$$\frac{dx}{dt} = -\frac{x}{\tau} + \mu \tag{2.10}$$

where $x = v$. Then,

$$x(t) = \mu\tau(1 - e^{-\frac{t}{\tau}}) \tag{2.11}$$

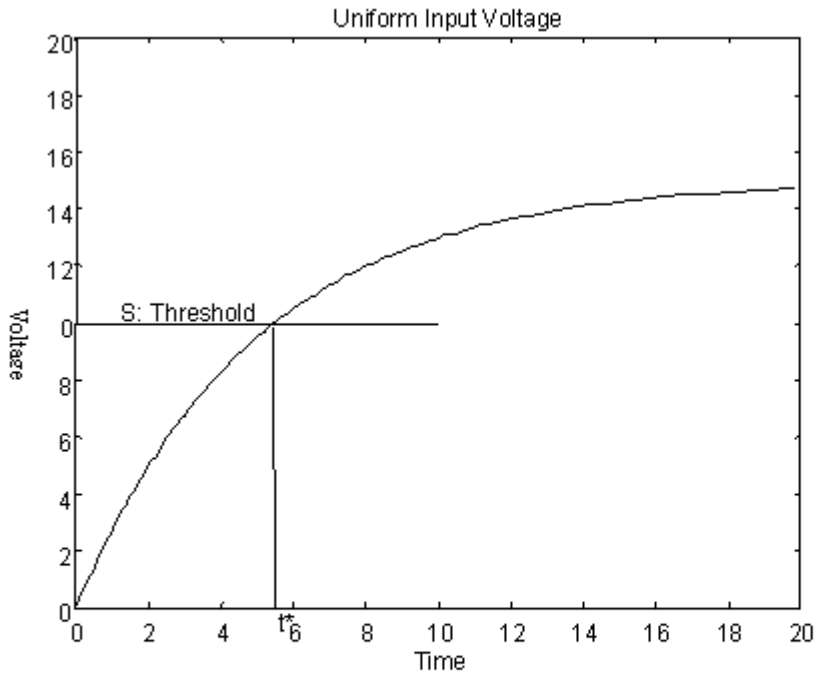

Figure 2.3. The trajectory of the membrane voltage with uniform input current. *The rest curve approaches asymptote which is the product of* μ *and* τ*, 15. The straight horizontal line is the threshold,* $S = 10$*. As we defined,* t^* *is the time at which mean of membrane voltage passes the threshold.*

We define t^* as the time at which mean of membrane voltage passes the

threshold. So,

$$t^* = -\tau log(1 - \frac{S}{\mu\tau}) \tag{2.12}$$

Figure 2.3 plotted by Matlab shows that the mean trajectory of voltage, where x_0 is 0, μ, uniform input current, is 3 $mvolt/msec$, τ, membrane constant, is 5 $msec$, S, threshold, is 10 $mvolt$. We obtain t^* is 5.4931 $msec$. Those values are reasonable parameters for neuron cell, in the spinal cord for example.

Equation 2.10 is easy to interpret. The more abstract OU process can be meaningfully derived. Equation 2.10 can arrive at the stochastic leaky integrator just by adding white noise

$$dx = (-\frac{x}{\tau} + \mu)dt + \sigma dW, \quad x(0) = 0, \tag{2.13}$$

where W is a standard Wiener process, μ is a constant measured in millivolt per unit time which represents the mean synaptic input signal resulting from the dendritic currents generated by sensory stimulation or the action potentials of other neurons. We assumed that the mean of input is constant corresponding to an average steady–state stimulation and σ is also a constant which scales the Wiener process. The time origin in Equation 2.13

is the moment of the previous firing of an action potential. In the case of suprathreshold stimulation, the model assumes that at each moment of firing, which is mimicked by reaching a firing threshold S, the membrane potential is reset to its initial value, $X_0 = 0$ [43]. Solving the stochastic differential equation, we can obtain

$$E[x(t)] = \mu\tau(1 - e^{-\frac{t}{\tau}}) \tag{2.14}$$

$$Var[x(t)] = \frac{\sigma^2\tau}{2}(1 - e^{-\frac{2t}{\tau}}) \tag{2.15}$$

The OU process has been studied in [2], [31], [32], [33], and [8]. Some sophisticated numerical methods for the first passage time problem have been developed. But, no analytical solution for the OU process is known.

2.3.2 Stein's model

Stein proposed a stochastic model for nerve–cell activity in the presence of random synaptic inputs in 1965 [38]. It is for single neuron firing which incorporates relatively many physiological characteristics of real neurons. Study

of the model and its modifications and generalizations have been one of the most common approaches to the theoretical study of neuronal activity, such as in [20], [35], [27], [16], [18], [42], and [46]. The inputs of Stein's model are divided into excitatory and inhibitory ones and follow Poisson processes. The heuristical stochastic differential equation is

$$\frac{dx}{dt} = -\frac{x}{\tau} + a_E \frac{dN_E}{dt} - a_I \frac{dN_I}{dt}, \tag{2.16}$$

where τ is membrane constant, N_E and N_I are independent simple Poisson processes with mean rates λ_E and λ_I. The trajectories of N_E and N_I have discontinuities of $+1$ each time an excitatory or inhibitory input arrives. Hence the derivatives dN_E/dt and dN_I/dt, which appear in Equation (2.16), consist of a collection of delta functions concentrated at the random arrival times of the synaptic inputs. When an excitatory input arrives, x will jump by $+a_E$ *mvolt*, whereas when an inhibitory input arrives x will jump by $-a_I$ *mvolt*. The mean and variance of the depolarization in Stein's model are [43]

$$E[x(t)] = \tau(a_E\lambda_E - a_I\lambda_I)(1 - e^{-\frac{t}{\tau}}), \tag{2.17}$$

and

$$Var[x(t)] = \frac{1}{2}\tau(a_E^2\lambda_E + a_I^2\lambda_I)(1 - e^{-\frac{2t}{\tau}}). \tag{2.18}$$

2.4 Approximation of the First Passage Time

To study the properties of the models themselves, approximation methods for model are very useful sometimes. Charles E. Smith summarized the approximation methods for the first passage time in [37] and [36]. We are interested in the case with deterministic crossing. The term "deterministic crossing" will be used when the mean voltage crosses a threshold, S. Our description is a simple generalization of the method for Stein's model. In this article, we also call it Stein's method. Let $r(t) = S - E[x(t)]$ be the recovery process following a spike, where S is the threshold. Besides requiring that the mean voltage crosses S, i. e. deterministic crossings, we require that

1. The membrane voltage distribution does not change its shape drastically near t^*.

2. The standard deviation of the FPT is considerably less than the corre-

lation time of $x(t)$ around t^*.

3. $r(t)$ is invertible and sufficiently smooth.

Let h be the inverse function of $r(t)$, that is , $h[r(t)] = t$. Then, a pdf of first passage time, $g(S, t|x_0)$, is approximately $f(x)|dh(x)/dx|$ evaluated at t^*, where $f(x)$ is the marginal distribution of $S - x(t^*)$. This is the usual Jacobian transformation of random variables, i. e., we are treating the membrane voltage process like a singular random process. For example, if $f(x)$ is Gaussian or normal and $r(t)$ is a decaying exponential, $g(S, t|x_0)$ is approximately lognormal.

In many cases, we may only be interested in the first few moments of the FPT. The function h is now expanded in a Taylor's series about $r(t^*)$. The approximations for the mean and variance are given next with $y = r(t)$, and μ_n is the nth central moment of the random variable $S - x(t^*)$ [29]:

$$E(t) \approx t^* + h''(y)\frac{\mu_2}{2!} + h'''(y)\frac{\mu_3}{3!} +, \cdots \tag{2.19}$$

$$Var(t) \approx (h')^2\mu_2 + h'h''\mu_3 - (h''\frac{\mu_2}{2!} + h'''\frac{\mu_3}{3!})^2 +, \cdots \tag{2.20}$$

where prime denotes differentiation with respect to membrane voltage. The expressions of the first four derivatives of $h[r(t)]$ are in the section 3.2.1 on page 35. Stein's original approximation method was the first term of Equations (2.19) and (2.20). Then,

$$E(t) = t^*, \tag{2.21}$$

and

$$Var(t) = \left[\frac{dx}{dt}\right]^2 Var[x(t)]. \tag{2.22}$$

We expect Stein's method to work in the OU process. There are a few reasons for us to consider it. In Stein's model in the previous section the membrane voltage is a discontinuous function of time. Just as the OU process in which the Wiener process is with drift can be viewed as a smoothed versions of Stein's model [43]. Or, the OU process can be constructed with the same first and second infinitesimal moments as the membrane voltage in Stein's model. This is also called usual diffusion approximation which has

been studied in [2], [32], [33], [17], [8], and [22].

Stein's method is expected to work for the OU process under some conditions. For example, we expect it to perform best when the excitatory post–synaptic potential (EPSP) and inhibitory post–synaptic potential (IPSP) amplitudes are small and input frequencies are large. The diffusion approximation therefore has infinitesimal mean

$$a_E\lambda_E - a_I\lambda_I - x \approx \mu - x, \quad a_E, a_I > 0, \tag{2.23}$$

and infinitesimal variance

$$a_E^2\lambda_E + a_I^2\lambda_I \approx \sigma^2. \tag{2.24}$$

Because Stein's method only uses one term of the Taylor's series, there is some limit for its application. It is reasonable to try more terms of the Taylor's series to see if it can improve this method. We hope that the parameter range will increase or get better approximation if we use more terms of the Taylor's series.

2.5 Distribution Comparison Method

The analysis of neural spike trains has a long history [43]. There are two main approaches for such analysis. The first is to formulate a stochastic model for the neuron's activity and inputs, derive the distribution of the FPT, and use it to fit the model to data. The stochastic process is often modelled as a random walk such as Stein's model or an diffusion model such as the OU process. Another important approach in such a study is to fit standard families of densities to the FPT, such as the lognormal or gamma, using maximum likelihood or some ad hoc technique. So, another trial is that we want to compare the approximated FPT distribution derived by using Stein's method with the lognormal distribution fitted for the simulated FPT of the OU process.

In many cases, there is not enough information to assume that the candidate families contain the true distribution that is generating the data. This is certainly the case for the problem at hand. So, we leave the true distribution for the FPT histograms unspecified; using the simulation data, we then seek to identify the distribution which is closer to the true and unknown distribution.

The approach here is based on the results of Foutz and Srivastava(1977)

[6], Nishii(1988) [28] and White(1982) [45]. We now describe the approach in general , and then specialize it to the case of the lognormal versus the approximated distribution. To assess the closeness of two densities f and p on the real line, we use Kullback–Leibler information criterion (or divergence)

$$I[p : f] = \int_0^\infty p(x) log \left[\frac{p(x)}{f(x)} \right] dx. \tag{2.25}$$

It is known that $I[p : f] \geq 0$, with equality only when $p = f$ [45]. For example, if $p(x) = \mu e^{-\mu x}$ and $f(x) = \lambda e^{-\lambda x}$ for $x > 0$ and zero otherwise, then $I[p : f] = \lambda/\mu - 1 - log(\lambda/\mu)$, which is 0.09 when the ratio of the means of these exponential densities is $\lambda/\mu = 1.5$. Next, if p and f are normal densities with means μ and ν, respectively, and both variances equal to 1, then $I[p : f] = (\mu - \nu)^2/2$, which is 0.125 when $|\mu - \nu| = 0.5$.

Kullback–Leibler information criterion is not a metric. But, it does have an advantage over metrics for the problem of comparing two approximations f_1 and f_2 to an unknown density p. Specifically,

$$I[p : f_1] - I[p : f_2] \;\; = \;\; \int_0^\infty p(x) log \left[\frac{f_2(x)}{f_1(x)} \right]$$

$$= \quad E_p \left[log \frac{f_2(Y)}{f_1(Y)} \right] \tag{2.26}$$

where E_p refers to expectation with respect to the density p, which generates the random variable Y. In practice, given independent and identically distributed data $(Y_1, \ldots, Y_n)$ from p, an estimate of E_p is

$$\frac{1}{n} \sum_{1}^{n} log \left[\frac{f_2(Y_i)}{f_1(Y_i)} \right]. \tag{2.27}$$

If this estimate is positive, we conclude that f_2 is closer to p than f_1.

Chapter 3

Methods

3.1 Simulation

In many physical problems involving random phenomena we are unable to find exact expressions (or sometimes even expressions) for quantities of interest. We may then turn to simulation in which the situation of interest is reproduced theoretically and the results are analyzed. Simulation, when performed accurately, can be a powerful method for approximating solutions for very complex problems. In order to evaluate if Stein's method and its modification will work in the OU process, I simulated Equation (2.13) using the input from a normal distribution with mean μ, and variance σ^2 with a

constant threshold S.

3.1.1 Testing for the Independence of Random Numbers

In the case of two random variables (X, Y), a random sample of size n consists of the n pairs (X_i, Y_i), $i = 1, 2, \ldots, n$. The sample correlation coefficient is often defined as

$$R = \frac{\sum_{i=1}^{n}(X_i - \bar{X})(Y_i - \bar{Y})}{\sqrt{(\sum_{i=1}^{n}(X_i - \bar{X})^2)(\sum_{i=1}^{n}(Y_i - \bar{Y})^2)}}, \tag{3.1}$$

where

$$\bar{X} = \frac{1}{n}\sum_{i=1}^{n} X_i$$

and

$$\bar{Y} = \frac{1}{n}\sum_{i=1}^{n} Y_i$$

are the sample means for X and Y [44]. Value of R close to zero indicates that X and Y are uncorrelated, which sometimes implies they are independent, for example, they are from a normal distribution. In the present situation we are concerned with a sequence of random variables $X_1, X_2, \ldots, X_n$. Considering pairs of consecutive variables $(X_1, X_2), (X_2, X_3), \ldots, (X_{n-1}, X_n)$, we

can regard the first member of each pair as one variable and the second member as another variable. The correlation coefficient of the first and second variables is called the serial correlation coefficient at lag 1:

$$R_1 = \frac{\sum_{i=1}^{n-1}(X_i - \bar{X}_*)(X_{i+1} - \bar{X}_{**})}{\sqrt{(\sum_{i=1}^{n-1}(X_i - \bar{X}_*)^2)(\sum_{i=1}^{n-1}(X_{i+1} - \bar{X}_{**})^2)}} \tag{3.2}$$

where

$$\bar{X}_* = \frac{1}{n-1}\sum_{i=1}^{n-1} X_i$$

is the mean of the first $n-1$ variables and

$$\bar{X}_{**} = \frac{1}{n-1}\sum_{i=1}^{n-1} X_{i+1}$$

is the mean of the last $n-1$ variables.

It is possible, however, that consecutive variables are independent. But, for example, the pairs $(X_1, X_3), (X_2, X_4), \cdots, (X_{n-2}, X_n)$, are not independent. Thus, we also compute a correlation coefficient for X_i and X_{i+2}. In general, the serial correlation coefficient at lag k when n is large is defined as

$$R_k = \frac{\sum_{i=1}^{n-k}(X_i - \bar{X})(X_{i+k} - \bar{X})}{\sum_{i=1}^{n}(X_i - \bar{X})^2}. \tag{3.3}$$

Furthermore, under the assumption of independence, R_k is, when n is large, providing $k \ll n$, approximately normal with mean zero and variance $1/n$. It is useful to plot R_k versus k to obtain a serial correlogram. Figure 3.1 shows that all values of R_k of the random numbers which our program generated by using Matlab lie in the interval of $[-1.96/\sqrt{n}, 1.96/\sqrt{n}]$, where n is 1000 and k is in the interval [1, 100]. Another way is to use the joint histogram. Figure 3.2 is the joint histogram of X_i and X_{i+1}. The joint histogram of two independent normal random variable has a symmetry "mountain" shape, just as shown in Figure 3.2. Figure 3.3 is the scatter plot of random number X_i against X_{i+1}. Those figures give the evidence for that X_i and X_{i+1} are independent.

3.1.2 Euler Method

As Equation (2.13) describes the time evolution of the trajectories of the membrane potential $x = \{x_t : t_0 \leq t \leq T\}$, a discretized version of it can

be obtained by a mesh of points t_i such that $t_0 < t_1 < \cdots < t_n = T$, and $t_{i+1} - t_i = \Delta t$. Equation (1.1) on $t_0 \leq t \leq T$ with the initial value $x_{t_0} = x_0$ can then be rewritten as

$$x(t_{i+1}) = x(t_i) + (-\frac{x(t_i)}{\tau} + \mu)(t_{i+1} - t_i) + \sigma(x(t_i), t_i)(W(t_{i+1}) - W(t_i)). \quad (3.4)$$

This is an Euler approximation which is a discrete time stochastic process $x(t)$ satisfying the iterative Equation (3.4). The procedure for solving Equation (1.1) is to compute $x(t_{i+1})$ from the knowledge of $x(t_i)$ realizing that the increments of the standard Wiener process

$$\Delta W_i = W_{i+1} - W_i \quad (3.5)$$

appearing in Equation (3.4) are mutually independent, normally distributed r.v.'s with mean zero and variance $(t_{i+1} - t_i)$ independent of $X(t_i)$ [15]. We use Matlab to generate random numbers of the increments of the Wiener process with mean $\mu = 0$ and variance $\sigma^2 = \Delta t$.

There are several sources of error in Euler's method that may make the approximation y_n to $y(x_n)$ in Equation (3.6) unreliable for large values of

n, those for which x_n is not sufficiently close to x_0. The error in the linear approximation formula

$$Y(x_{n+1}) \approx y_n + h \cdot f(x_n, y_n) = y_{n+1} \tag{3.6}$$

is the amount by which the tangent line at (x_n, y_n) departs from the solution curve through (x_n, y_n). This error, introduced at each step in the process, is called the local error in Euler's method. Besides local error, y_n itself suffers from the accumulated effects of all the local errors introduced at the previous steps. This is called cumulative error in Euler's method; it is the amount by which the polygonal stepwise path from (x_0, y_0) departs from the actual solution curve through (x_0, y_0). The usual way of attempting to reduce the cumulative error in Euler's method is to decrease the step h. But, we can not simply choose an exceedingly small step size and expect the very great accuracy of result. One obvious reason is the time required for the computation. The second reason is more subtle. In addition to the local and cumulative errors discussed previously, the computer itself will contribute roundoff error at each step because only finite number of significant digits can be used in each calculation. An Euler's method computation with $h = 0.0001$

will introduce roundoff errors 1000 times as often as one with $h = 0.1$ [5]. In our study, we choose $h = 0.1$ to do the simulation.

The average time for the sample path of $x(t)$ to approach to its asymptote is about 20 $msec$ (see Figure 2.3). Because the ΔT we will use is 0.1 $msec$, to make sure that all the sample path of $x(t)$ to approach to its asymptote in our program, we let t_n be 100 $msec$ which is much greater than the average time for the sample path of $x(t)$ to approach to its asymptote. So, n in our program is 1000.

3.1.3 Parameter

For any quantitative discussion about the models and their mutual comparison, at least the approximation about their parameters is necessary. The most appropriate would be to estimate these parameters from the data recorded intracellularly according to the model construction. So, we use reasonable parameters of a neuron in the spinal cord for μ, τ and S. For the Wiener process parameter σ^2 we can only speculate. From the diffusion approximation in Equations (2.23) and (2.24), we can approximate σ by the amplitudes of excitatory and inhibitory postsynaptic potentials and their input rates λ_E and λ_I which have a wide range. More information about the

Wiener parameters in the OU process comes immediately from the experimental data in [11], where direct estimation from FPT has been performed. In their paper the estimated values of the parameter σ goes up to 15. We also referred to parameter values in [3], [41], [42], and [24] to pick the σ values which are shown in Table 3.1.

Table 3.1. Parameter values used in this study.

Parameter	Value	Units
τ	5	$msec$
μ	3	$mvolt/msec$
σ	varies (0.5, 2, 4)	$mvolt/msec$
S	varies (6–14)	$mvolt$

3.1.4 Goodness–of–fit–test

When we decide on basis of data which of probability distribution to use for membrane voltage at the specific time or the FPT of the OU process, common way to approach this problem is to construct a histogram or stem–and–leaf display. Histograms and stem–and–leaf displays will give a visual impression of the shape of the data set, but they are not adequate tools for discrimination. There are several statistical tests, such as goodness–of–fit

tests, which test the null hypothesis that the distribution is in some specified form. We use the D test developed by D'Agostino in 1971. It is one of most powerful tests available for detecting departures from a hypothesized normal or lognormal density function when n is between 50 and 1000. D'Agostino shows that his test compares favorably with other tests in its ability to reject H_0, when H_0 is actually false.

Suppose we wish to test the null hypothesis that the underlying distribution is normal. Then the D test is conducted as follows:

1. Draw a random sample $x_1, x_2, \ldots, x_n$ of size $n \geq 50$ from the population of interest. n is 400 in this study.

2. Order the n data from smallest to largest to obtain the sample order statistics $x_{[1]} \leq x_{[2]} \leq \ldots \leq x_{[n]}$.

3. Compute the statistic

$$D = \frac{\sum_{i=1}^{n}[i - \frac{1}{2}(n+1)]x_{[i]}}{n^2 s}, \tag{3.7}$$

where

$$s = \left[\frac{1}{n} \sum_{i=1}^{n} (x_i - \bar{x})^2 \right]^{1/2} . \tag{3.8}$$

4. Transform D to the statistic Y by computing

$$Y = \frac{D - 0.28209479}{0.02998598/\sqrt{n}} \tag{3.9}$$

   If n is large and the data are drawn from a normal distribution, then the expected value of Y is zero. For nonnormal distributions Y will tend to be either less than or greater than zero, depending on the particular distribution.

5. Reject at the α significance level the null hypothesis that the n data were drawn from a normal distribution if Y is less than the $\alpha/2$ quantile or greater than the $1 - \alpha/2$ quantile of the distribution of Y. For $n = 400$, and $\alpha = 0.05$, the upper and lower limit are 1.633 and -2.270, respectively [7].

The Y statistic can also be used to test the null hypothesis of a lognormal population by using $y_i = log(x_i)$ in place of x_i in the calculation.

3.2 Approximation

First, we go to the details of approximating the first two moments of the FPT (mean and variance).

3.2.1 Approximation of Moments of the FPT

• The First Four Derivatives of $h[r(t)]$

$h[r(t)] = t$, i. e., $h(x)$ is the inverse function of $r(t)$. Recall that the first derivative of an inverse function can be expressed as the reciprocal of the derivative of the original function [40]. Then, we take derivative of the first order derivative to get second order derivative, and so on.

$$h'[r(t)] = [r'(t)]^{-1} \tag{3.10}$$

$$h''[r(t)] = -[r'(t)]^{-3} r''(t) \tag{3.11}$$

$$h'''[r(t)] = 3[r'(t)]^{-5}[r''(t)]^2 - r'''(t)[r'(t)]^{-4} \tag{3.12}$$

$$h''''[r(t)] = -15[r'(t)]^{-7}[r''(t)]^3 + 10[r'(t)]^{-6} r''(t) r'''(t) - r''''(t)[r'(t)]^{-5} \tag{3.13}$$

•The First four derivatives of r(t*)

The First Four Derivatives of $h[r(t)]$ evaluated at t^* at which the mean of $x(t)$ passes the threshold S. We can get the following by taking derivatives to $r(t)$ and plugging in $t^* = -\tau log(1 - \frac{s}{\mu\tau})$ to $r(t)$.

$$r'(t) = -\mu e^{\frac{-t}{\tau}} \quad , \quad r'(t^*) = -(\mu - \frac{s}{\tau}) \tag{3.14}$$

$$r''(t) = \frac{\mu}{\tau} e^{\frac{-t}{\tau}} \quad , \quad r''(t^*) = \frac{1}{\tau}(\mu - \frac{s}{\tau}) \tag{3.15}$$

$$r'''(t) = -\frac{\mu}{\tau^2} e^{\frac{-t}{\tau}} \quad , \quad r'''(t^*) = -\frac{1}{\tau^2}(\mu - \frac{s}{\tau}) \tag{3.16}$$

$$r''''(t) = \frac{\mu}{\tau^3} e^{\frac{-t}{\tau}} \quad , \quad r''''(t^*) = \frac{1}{\tau^3}(\mu - \frac{s}{\tau}) \tag{3.17}$$

After substituting to the derivatives of $h[r(t)]$, we can obtain

$$h'(t^*) = -(\mu - \frac{s}{\tau})^{-1} \tag{3.18}$$

$$h''(t^*) = \frac{1}{\tau}(\mu - \frac{s}{\tau})^{-2} \tag{3.19}$$

$$h'''(t^*) = -\frac{2}{\tau^2}(\mu - \frac{s}{\tau})^{-3} \tag{3.20}$$

$$h''''(t^*) = \frac{6}{\tau^3}(\mu - \frac{s}{\tau})^{-4} \tag{3.21}$$

• The nth central moment (μ_n) of the normal distribution $N(\mu, \sigma^2)$

If n is odd, the moment is 0 due to the symmetry of the distribution. If

n is even, $n = 2k$, the following is the formula for it.

$$E[(x-\mu)^{2k}] = \frac{(2k)!\sigma^{2k}}{k!2^k} \tag{3.22}$$

So, $\mu_3 = \mu_5 = 0$ and $\mu_4 = 3\sigma^4$, $\mu_6 = 15\sigma^6$.

• The Taylor's series of $h[r(t)]$

$$E(t) = t^* + h''\frac{\mu_2}{2!} + h'''\frac{\mu_3}{3!} + h''''\frac{\mu_4}{4!} + \ldots + h^n\frac{\mu_n}{n!} \tag{3.23}$$

where u_n is nth central moment of $S - x(t^*)$.

• The Taylor's series of the variance of $h[r(t)]$

As we know

$$Var(t) = Var[h(r(t))] = E(h(r(t))^2) - [E(h(r(t)))]^2. \tag{3.24}$$

letting $g(t) = [h(r(t))]^2$, we can write $E([h(r(t^*))]^2)$ as

$$E([h(r(t^*))]^2) = g(t^*) + g''(t^*)\frac{\mu_2}{2!} + g'''(t^*)\frac{\mu_3}{3!} + g''''(t^*)\frac{\mu_4}{4!} + \ldots + g^n(t^*)\frac{\mu_n}{n!} \tag{3.25}$$

The first four derivatives of $g(t)$ are

$$\begin{aligned} g'(t) &= 2h(t)h'(t) = 2hh' && (3.26)\\ g''(t) &= 2[h'(t)]^2 + 2h(t)h''(t) = 2h'^2 + 2hh'' && (3.27)\\ g'''(t) &= 6h'(t)h''(t) + 2h'''(t)h(t) = 6h'h'' + 2h'''h && (3.28)\\ g''''(t) &= 6[h''(t)]^2 + 8h'(t)h'''(t) + 2h''''(t)h(t) \\ &= 6h''^2 + 8h'h''' + 2h''''h && (3.29) \end{aligned}$$

If we use the original Stein's method to do the approximation, the mean and variance of FPT are

$$E(t) = -\tau log(1 - \frac{s}{\mu\tau}) \tag{3.30}$$

and

$$Var(t) = \frac{1}{2}\frac{\tau S(2\mu\tau - S)}{(\mu\tau - S)^2\mu^2}\sigma^2. \tag{3.31}$$

If we use the first two terms to do the approximation, the mean of FPT is

$$E(t) = t^* + h''\frac{\mu_2}{2!} = -\tau log(1 - \frac{s}{\mu\tau}) + \frac{1}{4}\frac{S(2\mu\tau - S)}{(\mu\tau - S)^2\mu^2}\sigma^2 \tag{3.32}$$

For the variance of FPT we need to calculate the $E[h^2(r(t^*))]$ and $[E(h(r(t^*)))]^2$,

$$E[h^2(r(t^*))] = h^2 + (2h'^2 + 2h''h)\frac{\mu_2}{2!} \tag{3.33}$$

$$[E(h(r(t^*)))]^2 = (h + h''\frac{\mu_2}{2!})^2, \tag{3.34}$$

where h is $h[r(t^*)]$. So, the variance of FPT is

$$\begin{aligned} Var(t) &= E([h(r(t^*))]^2) - [E(h(t^*))]^2 \\ &= h'^2\mu_2 - \frac{h''^2\mu_2^2}{4}. \end{aligned} \tag{3.35}$$

Then we plug in $h(r(t^*))$ and obtain

$$Var(t) = \frac{\tau^2}{(\mu\tau - S)^2}\sigma_x^2 - \frac{\tau^2}{4(\mu\tau - s)^4}\sigma_x^4. \tag{3.36}$$

where σ_x^2 is $Var[x(t^*)]$,

$$\sigma^2(x) = \frac{\sigma^2 s}{\mu} - \frac{\sigma^2 s^2}{2\mu^2\tau} = \frac{s(2\mu\tau - s)}{2\mu^2\tau}\sigma^2. \tag{3.37}$$

So, the variance of FPT can be written as

$$Var(t) = \frac{S(2\mu\tau - S)^2}{2\mu^2(\mu\tau - S)}\sigma^2 - \frac{S^2(2\mu\tau - S)^4}{4\mu^4(\mu\tau - S)^4}\sigma^4 \tag{3.38}$$

If we use first four terms to do the approximation, then the mean of FPT is

$$\begin{aligned} E(t) &= t^* + h''\frac{\mu_2}{2!} + h'''\frac{\mu_3}{3!} + h''''\frac{\mu_4}{4!} \\ &= -\tau log(1 - \frac{s}{\mu\tau}) + \frac{1}{4}\frac{S(2\mu\tau - S)}{(\mu\tau - S)^2\mu^2}\sigma^2 + \frac{3}{16}\frac{S^2(2\mu\tau - S)^2}{\tau(\mu\tau - S)^4\mu^4}\sigma^4 \end{aligned} \tag{3.39}$$

For the variance of FPT, the calculation steps are as following,

$$E[h^2(r(t^*))] = h^2 + (2h'^2 + 2h''h)\frac{\mu_2}{2!} + (6h'h'' + 2h'''h)\frac{\mu_3}{3!} + (6h''^2 + 8h'h''' + 2h''''h)\frac{\mu_4}{4!} \tag{3.40}$$

$$[E(h(r(t^*)))]^2 = (h + h''\frac{\mu_2}{2!} + h'''\frac{\mu_3}{3!} + h''''\frac{\mu_4}{4!})^2 \tag{3.41}$$

So,

$$\begin{aligned} Var(t) &= E([h(r(t^*))]^2) - [E(h(t^*))]^2 \\ &= h'^2\mu_2 + h'h''\mu 3 + (6h''^2 + 8h'h''')\frac{\mu_4}{24} - \Big(\frac{h''^2\mu_2^2}{2^2} + \frac{h'''^2\mu_3^2}{6^2} + \frac{h''''^2\mu_4^2}{24^2} \\ &\quad +2h'''h''''\frac{\mu_3\mu_4}{6\times 24} + 2h''h'''\frac{\mu_2\mu_3}{2\times 6} + 2h''h''''\frac{\mu_2\mu_4}{2\times 24}\Big) \end{aligned} \tag{3.42}$$

$$Var(t) = \frac{\tau^2}{(\mu\tau - s)^2}\sigma_x^2 + \frac{5\tau^2}{2(\mu\tau - s)^4}\sigma_x^4 - \frac{3\tau^2}{4(\mu\tau - s)^6}\sigma_x^6 - \frac{9\tau^2}{16(\mu\tau - s)^8}\sigma_x^8 \tag{3.43}$$

$$Var(t) = \frac{s(2\mu\tau - s)\tau}{2(\mu\tau - s)^2\mu^2}\sigma^2 + \frac{5s^2(2\mu\tau - s)^2}{8(\mu\tau - s)^4\mu^4}\sigma^4 - \frac{3s^3(2\mu\tau - s)^3}{32(\mu\tau - s)^6\tau^2\mu^6}\sigma^6 - \frac{9s^4(2\mu\tau - s)^4}{256(\mu\tau - s)^8\tau^2\mu^8}\sigma^8 \tag{3.44}$$

3.2.2 Confidence Limits for the mean and variance of Lognormal Distribution

There are several methods for calculating confidence limits. They are given in [7]. We use a simple method to estimate the mean μ and variance σ^2 of the two–parameter lognormal distribution. Suppose X is random variable of lognormal distribution, let $Y = log(X)$, so,

$$\bar{y} = \frac{1}{n}\sum_{i=1}^{n} y_i \tag{3.45}$$

$$s_y^2 = \frac{1}{n-1}\sum_{i=1}^{n}(y_i - \bar{y})^2. \tag{3.46}$$

Then, we replace μ_y and σ_y^2 by $\bar{y}$ and s_y^2 in the formulas for the true and unknown μ and σ^2. We get

$$\hat{\mu} = e^{\left(\bar{y}+\frac{s_y^2}{2}\right)} \tag{3.47}$$

and

$$\hat{\sigma}^2 = \hat{\mu}^2[e^{s_y^2} - 1] \tag{3.48}$$

There are also several methods for calculating confidence limits for mean of lognormal distribution. Land's method is considered as the best one. Land showed that the upper one-sided $100(1-\alpha)\%$ and the lower one-sided $100\alpha\%$ confidence limits for μ are obtained by calculating

$$UL_{1-\alpha} = e^{\left(\bar{y}+0.5s_y^2+\frac{s_y H_{1-\alpha}}{\sqrt{n-1}}\right)} \tag{3.49}$$

and

$$LL_{\alpha} = e^{\left(\bar{y}+0.5s_y^2+\frac{s_y H_{\alpha}}{\sqrt{n-1}}\right)}, \tag{3.50}$$

respectively, where $\bar{y}$ and s_y^2 are calculated using Equations (3.45) and (3.46), respectively. The quantities $H_{1-\alpha}$ and H_{α} are obtained from the tables provided by Land in [7]. In our study, we use $\alpha = 0.05$.

As to the confidence interval of variance of FPT, we just run the program

in a 100 time loop and get a sample of the variance. Then, we take the 97.5 percentile of the sample data as the upper confidence limit and 2.5 percentile of the sample data as the lower confidence limit. We repeat the procedure 10 times and obtain 10 confidence limits. We take the mean of the 10 percentiles as confidence limits of the variance.

We use the relationship between the approximation values of the mean and variance of FPT and the confidence interval of the simulatied mean and variance to tell if the approximation values are close enough to the simulation results. We conclude the approximation can work for those parameters if the approximation values fall in the confidence interval of the simulation data.

3.2.3 Approximation Error

If all the approximation values fall in the confidence interval no matter how many terms we used to approximate the mean and variance of FPT, we use the error of the approximation to tell which approximation is closer to the simulation data. It is defined as [42]:

$$E = \frac{Approximation - Simulation}{Simulation}(100\%)$$

$$= \quad \left(\frac{Approximation}{Simulation} - 1\right) 100\%. \tag{3.51}$$

We use the mean and standard deviation of 100 E values for all the approximation value to estimate which approximation method is better.

3.2.4 Approximation of Probability Density Function of the FPT

The marginal distribution of $x(t)$ is normal distribution with mean $E(x(t))$, which is $\mu\tau(1-e^{-\frac{t}{\tau}})$, and variance $\sigma^2\tau(1-e^{-\frac{2t}{\tau}})/2$. Then, the marginal distribution for $x(t^*)$ is $N(-\tau log(1-\frac{s}{\mu\tau}), \frac{s(2\mu\tau-s)}{2\mu^2\tau}\sigma^2)$. Obviously, $E(x(t^*)) = S$. So, the marginal distribution for $y = S - x(t^*)$ is $N(0, \frac{s(2\mu\tau-s)}{2\mu^2\tau}\sigma^2)$.

$$f_Y(y(t^*)) = \frac{1}{\sqrt{\frac{2\pi s(2\mu\tau-s)}{2\mu^2\tau}\sigma^2}} e^{-\frac{(y)^2}{\frac{s(2\mu\tau-s)}{s\mu^2\tau}\sigma^2}} \tag{3.52}$$

The pdf of FPT $g(s,t|x_0)$ is

$$g(s,t|x_0) = f_{Y_{t*}}(y) / \left|\frac{dh(y)}{dy}\right|, \tag{3.53}$$

where

$$y = r(t) = S - E(x(t)) = \mu\tau(1 - e^{-\frac{t}{\tau}}). \tag{3.54}$$

and $h'(y) = h'(r(t)) = -\mu e^{-\frac{t}{\tau}}$. So, the pdf of FPT approximated by using Stein's method (Jacobian transform) is

$$g(s,t|x_0) = \frac{\mu e^{-\frac{t}{\tau}} e^{-\frac{(\mu\tau(1-e^{-\frac{t}{\tau}})-S)^2}{\sigma^2\tau(1-(1-\frac{S}{\mu\tau})^2)}}}{\sqrt{\pi\sigma^2\tau(1-(1-\frac{S}{\mu\tau})^2)}}, \tag{3.55}$$

where $t \in (0, \infty)$.

The lognormal pdf estimated from simulation data is

$$f_T(t) = \frac{1}{t\sigma_{log(t)}\sqrt{2\pi}} e^{-\frac{(log(t)-\mu_{log(t)})^2}{2\sigma^2_{log(t)}}} \tag{3.56}$$

where $t \in (0, \infty)$, $\mu_{log(t)}$ is the mean of $log(t)$ and $\sigma^2_{log(t)}$ is the variance of $log(t)$.

3.3 Comparison of Two Probability Density Functions

We use Stein's method to approximate the probability density function of the FPT. We estimate the lognormal density function by using the maximum likelihood estimator [4]. Then, we can see which one is better for the simulation data by Kullback–Leibler information criteria.

First, we describe the general comparison of two probability density functions. We define

$$F = \{f(y|\alpha) : \alpha \in A\} \tag{3.57}$$

and

$$G = \{f(y|\beta) : \beta \in B\} \tag{3.58}$$

be two families of densities under consideration, and let $p(y)$ denote the true and unknown density that is generating the data. We let α_* be the quasi–true parameter in A associated with the true density $p(y)$. Then $f(y|\alpha_*)$ is

the member of F that minimizes $I[p : f(\cdot|\alpha)]$, over $\alpha \in A$, and define $\beta_* \in B$ similarly. Thus,

$$I_F = I_{F[p:a_*]} = \int_0^\infty p(y) log \left[\frac{p(y)}{f(y|a^*)} \right] dy \tag{3.59}$$

characterizes the proximity of F to p, and $I_G = I_G[p : \beta_*]$ (defined similarly) characterized the proximity of G to p. Thus, the difference

$$I_G - I_F = \int_0^\infty p(y) log \left[\frac{f(y|\alpha_*)}{g(y|\beta_*)} \right] dy \tag{3.60}$$

allows for a comparison of F and G, using estimates of α_* and β_*, which we describe next.

Given a random sample $Y = (y_1, \ldots, y_n)$ generated from $p(y)$, let the quasi–log–likelihood function of α under F be

$$L_n(\alpha|Y) = \sum_{i=1}^{n} log[f(y_i|\alpha)] \tag{3.61}$$

and a quasi–maximum likelihood estimator (QMLE) $\hat{\alpha}_n$ be a value which maximizes $L_n(\alpha|Y)$ over $\alpha \in A$; for G, define $L_n(\beta|Y)$ and $\hat{\beta}_n$ similarly.

A natural estimate of $I_G - I_F$ is

$$T_n = \frac{1}{n}\sum_{i=1}^{n} log\left[\frac{f(y_i|\hat{\alpha}_n)}{g(y_i|\hat{\beta}_n)}\right], \tag{3.62}$$

which is asymptotically normal:

$$\sqrt{n}[T_n - (I_G - I_F)] \rightarrow N(0, \sigma^2), \tag{3.63}$$

where the variance $\sigma^2 = E_p\left[log[f(Y|\alpha_*)/g(Y|\beta_*)]\right]^2$ is estimated by

$$\hat{\sigma^2} = \frac{1}{n}\sum_{i=1}^{n}\left[log\frac{f(y_i|\hat{\alpha}_n)}{g(y_i|\hat{\beta}_n)}\right]^2. \tag{3.64}$$

The regularity conditions that guarantee the existence of the quasi–true parameters α_* and β_*, the consistency of $\hat{\sigma}_n^2$ are described in the papers by [6], [45], and [28]. These conditions are satisfied for the comparison below. We omit the details of that verification.

The decision about which of the families, F or G, is closer to the true and unknown distribution $p(y)$, now proceeds in the following way. We first pose the null hypothesis $H_0 : I_G = I_F$ against the alternative hypothesis

$H_1 : I_G \neq I_F$. We then compute the statistic $\sqrt{n}T_n$ and its estimated standard deviation $\hat{\sigma}_n$. Given a confidence coefficient α, we construct the approximate confidence interval for $(I_G - I_F)$,

$$I_{n,\alpha} = \left(T_n + c_\alpha \frac{\hat{\sigma}_n}{\sqrt{n}}, T_n - c_\alpha \frac{\hat{\sigma}_n}{\sqrt{n}} \right) \tag{3.65}$$

where c_α is the upper $100(1-\alpha/2)$ percent point of the standard normal distribution (if $\alpha = 0.05, c_\alpha = 1.96$). If $0 \in I_{n,\alpha}$, then we cannot reject the null hypothesis that the two distributions are equally close to the true distribution; otherwise we reject the null hypothesis. Furthermore, if $I_{n,\alpha} \subseteq (0, \infty)$, we conclude that F is closer to the true model; if $I_{n,\alpha} \subseteq (0, -\infty)$, we conclude that G is closer to the true distribution. We now turn to the specifics for lognormal distribution. The QMLEs $\hat{\alpha}_n = (\hat{\alpha}_{1n}, \hat{\alpha}_{2n})$ for lognormal are obtained from Equations (3.66) and (3.67).

$$\hat{\alpha}_{1n} = \frac{1}{n} \sum_{1}^{n} log(y_i) \tag{3.66}$$

$$\hat{\alpha}_{2n} = \frac{1}{n} \sum_{1}^{n} [log(y_i) - \hat{\alpha}_{1n}]^2 \tag{3.67}$$

respectively. We already have the approximated density function derived from Stein's method. So, we can use the above method to compare them.

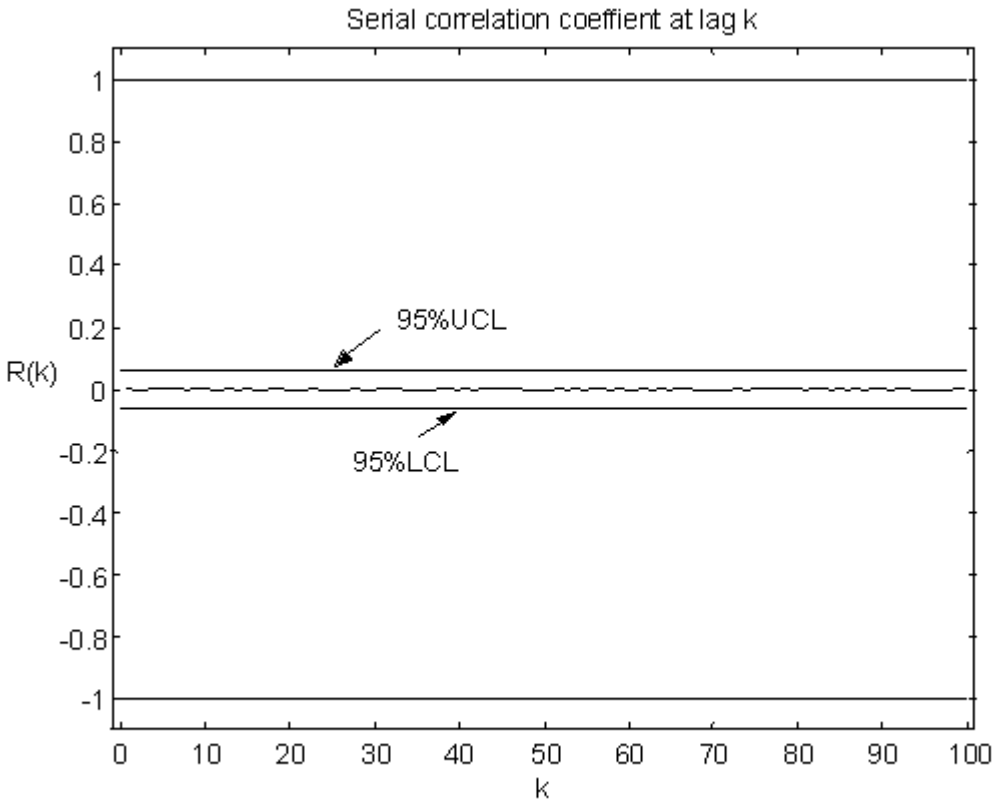

Figure 3.1. Serial correlation coefficient at lag k with n is 1000. *k is between [1,100]. The central irregular line is R_k. The two straight lines are upper confidence limit and lower confidence limit, respectively, as labelled. The random numbers are generated from a standard normal distribution with mean 0, and variance 1.*

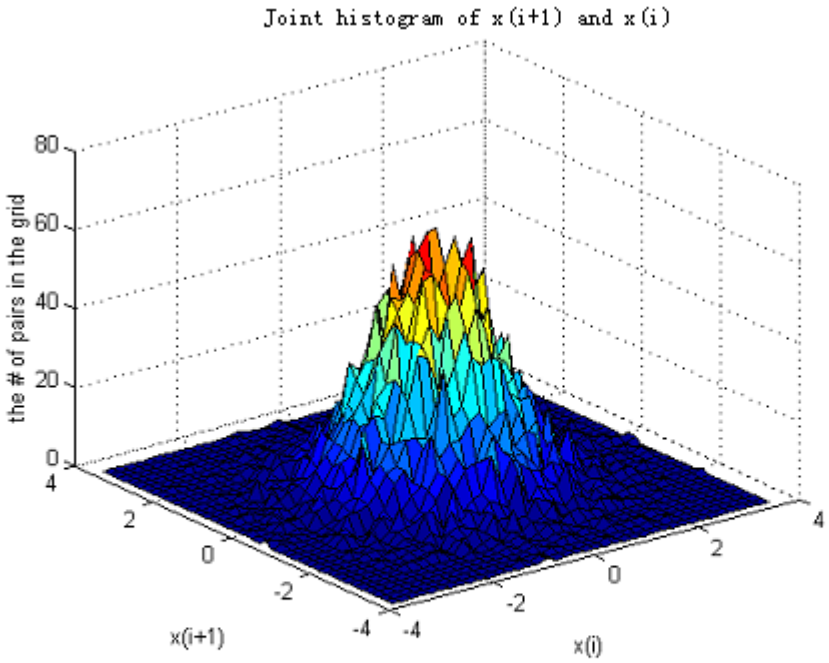

Figure 3.2. The joint histogram of random numbers X_i and X_{i+1}, where i represents the ith number generated by Matlab with n 1000.

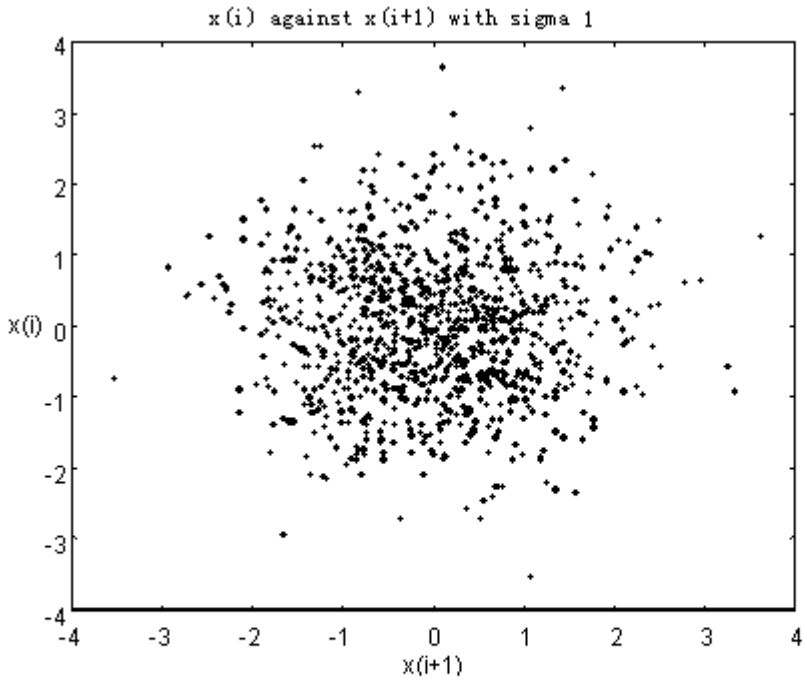

Figure 3.3. Scatter plot of the random numbers: X_{i+1} against X_i with n 1000. *The sigma is the standard deviation of the random numbers.*

Chapter 4

Results

4.1 Simulation

1. **The correlation time of the OU process** .

   Figures 4.1, 4.2, and 4.3 show that the correlation of the membrane voltage at different times. Clearly, variables x_6 and x_5 are highly correlated (the subscript represents time, $msec$), while variables x_{10} and x_5 are only slightly correlated, and variables x_{15} and x_5 are rarely correlated. The autocorrelation function in Figure 4.4 gives more detailed information on the correlation of the membrane voltages at different times. It also shows that the correlation time constant for the OU

process (at least 5 $msec$) is greater than the standard deviations of the corresponding FPT. The largest standard deviation of the FPT is 2.5 $mesc$, when the threshold is 14 $mvolt$. Most are less than 1 $msec$. This could also be obtained from the Stein's approximation method, in section 2.4 on page 18. Thus, the OU process has a long correlation time compared to the resultant standard deviation of FPT.

From the sample paths in Figures 4.5, 4.6, and 4.7, we can see the sample paths are always on one side of the expected mean membrane voltage for a while before they cross their expected mean. The correlation of the membrane voltage is apparent over short time ranges.

2. **The marginal distribution of membrane voltage is the normal distributed.**

   Figures 4.8, 4.9, and 4.10 show that the marginal distribution of x(t) is close to normal. The smooth curves are the pdfs of a normal distribution, which are estimated by using the method of moments, see [4] for details. The curve fitted from simulation data is very close to the expected curve. This suggests that the simulation results are quite close to the theoretical values. The goodness–of–fit tests give this evidence too. The Y values for the different times are in Table 4.1. Table 4.1.

D'Agostino's test results for the marginal distribution of $x(t)$.

time	5	10	15	20	25	30	35
Y	0.5172	0.3746	0.8196	0.6536	1.5296	1.8049	0.9387

The sample size of the $x(t)$ is 400. All the Y values are in the interval (-2.270,1.633). So, we do not reject the null hypothesis and conclude that all the variables $x(t)$ follow normal distribution.

3. **The lognormal distribution is very close to the distribution of FPT.**

   Figure 4.11 shows that both the normal distribution and the lognormal distribution provide a good fit to the histogram of the simulated FPT, when σ is 0.5. However, for the large values of the Wiener parameter, 4 and 16, Figures 4.12 and 4.13 show that only the lognormal family fit well. This suggests that for large Wiener parameter in the OU process, lognormal distribution is very close to the true distribution the FPT follows. The Y values of D'Agostino's test results are in Table 4.2 and give more evidence on this. We select threshold 7 *mvolt*, 10 *mvolt*, and 13 *mvolt* as examples.

Table 4.2. D'Agostino's test results for distribution of the FPT.

Threshold, S	σ		
mvolt	0.5	2	4
7	-1.6975	-0.2848	0.8183
10	-1.4606	0.0411	1.5692
13	-1.0100	0.3651	0.8468

The sample size of the FPT is 400. All the Y values are in the interval (-2.270, 1.633). So, we do not reject the null hypothesis and conclude that the variables FPT follow lognormal distribution.

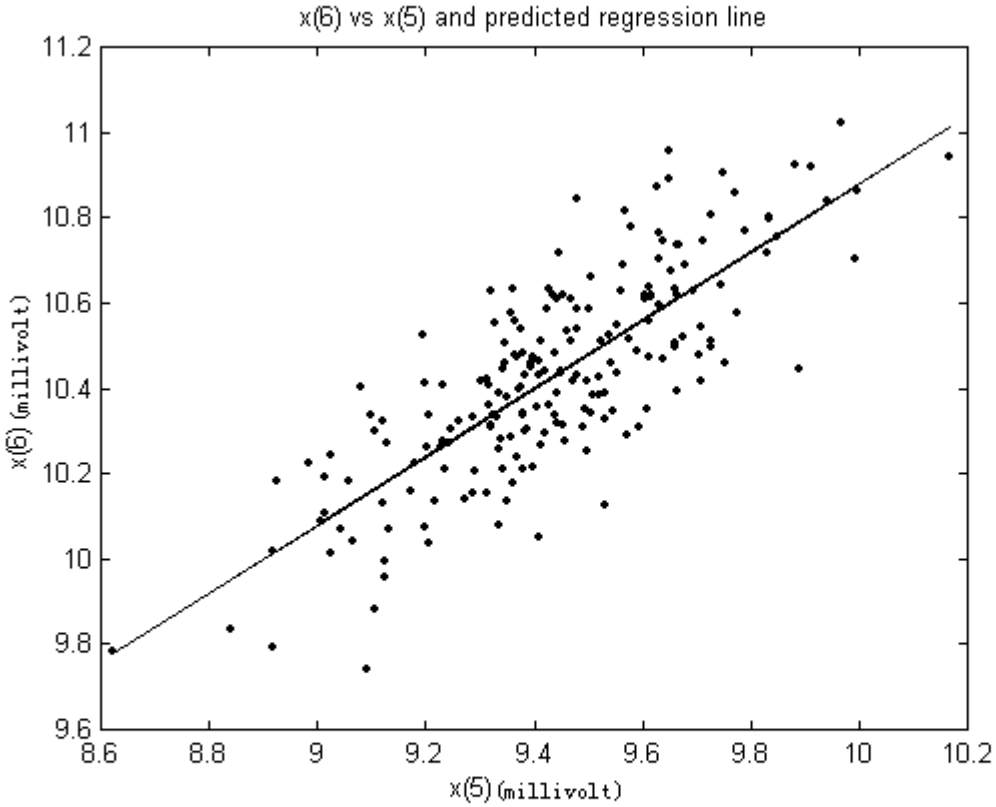

Figure 4.1. The scatter plot of membrane voltage at 6 *msec* versus that at 5 *msec* and the regression line. *The sample size of the membrane voltage at different time is 200.*

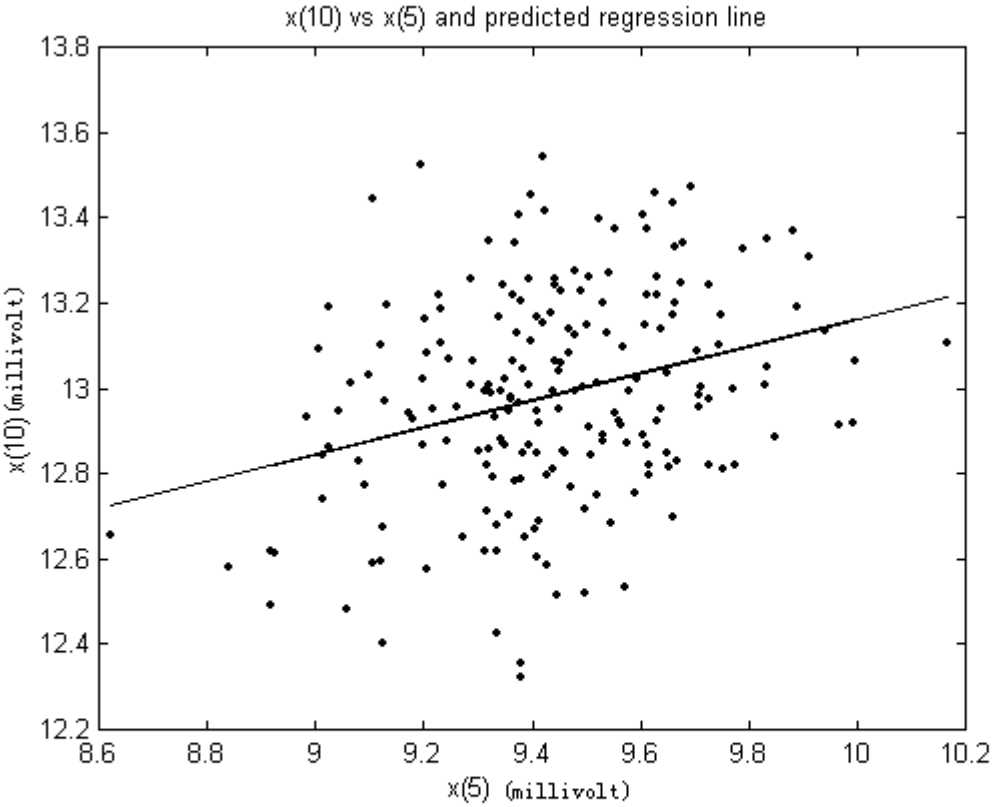

Figure 4.2. The scatter plot of membrane voltage at 10 *msec* versus that at 5 *msec* and the regression line.

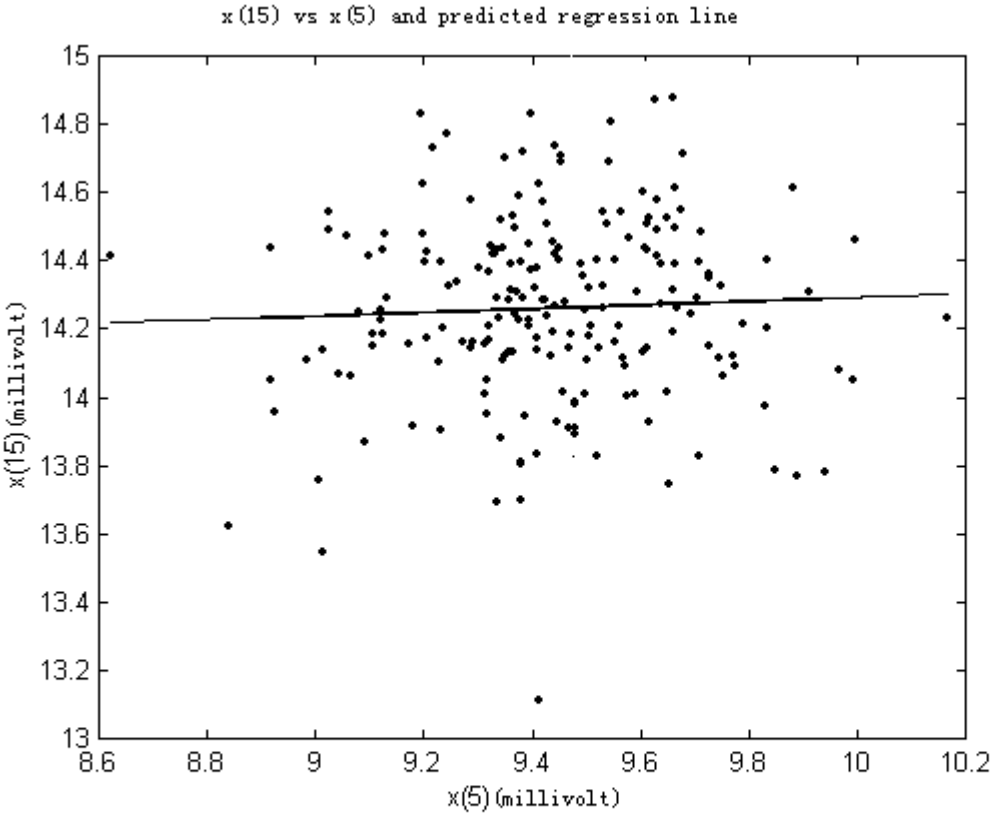

Figure 4.3 The scatter plot of membrane voltage at 15 *msec* versus that at 5 *msec* and the regression line.

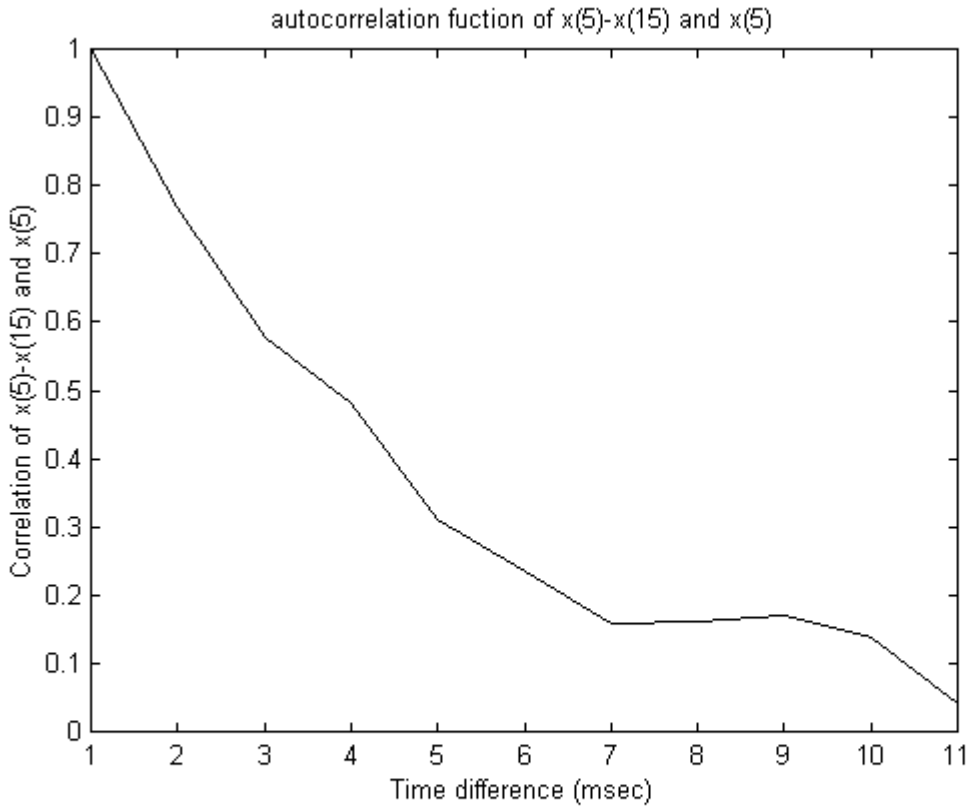

Figure 4.4. The autocorrelation function of the membrane voltage from 5 *msec* to 15 *msec*. *x-axis represents the time difference.*

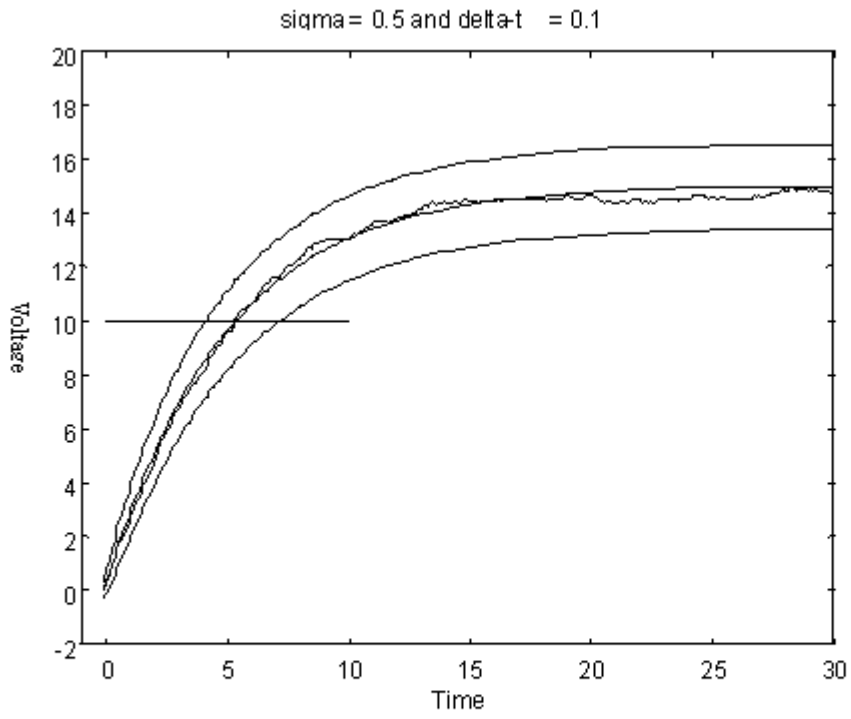

Figure 4.5. A sample path of the membrane voltage with the Wiener process parameter 0.25 (the irregular curve). *The central smooth curve is the expected mean of membrane voltage and the two smooth curves beside it are the upper and lower 95% confidence limit, respectively. The horizontal line represents the threshold 10 mvolt.*

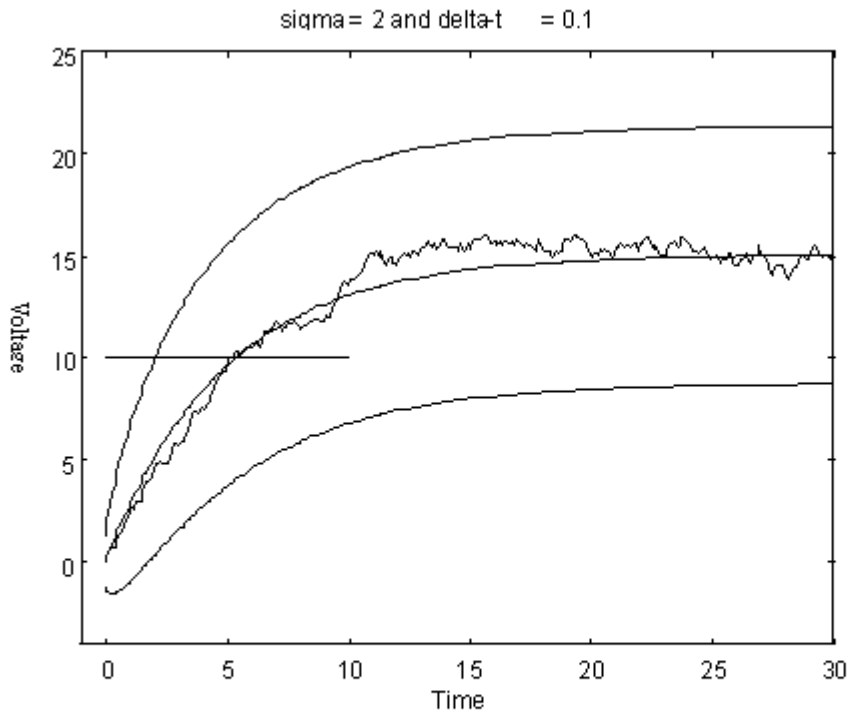

Figure 4.6. A Sample path of the membrane voltage with the Wiener process parameter 4 (the irregular curve). *The central smooth curve is the expected mean of membrane voltage and the two smooth curves beside it are the upper and lower 95% confidence limit, respectively. The horizontal line represents the threshold 10 mvolt.*

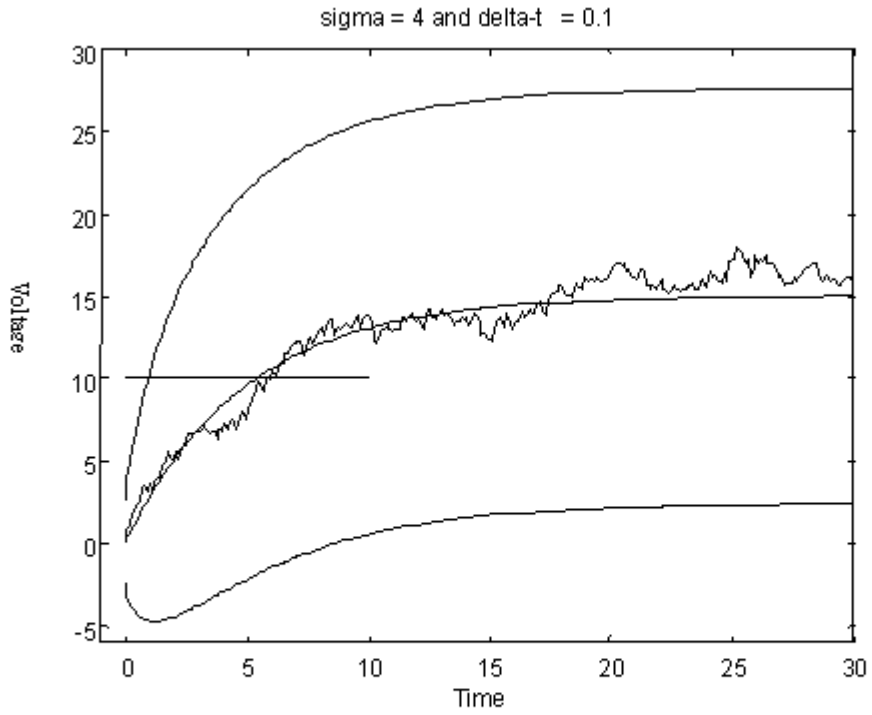

Figure 4.7. A Sample path of the membrane voltage with the Wiener process parameter 16 (the irregular curve). *The central smooth curve is the expected mean of membrane voltage and the two smooth curves beside it are the upper and the lower 95% confidence limit, respectively. The horizontal line represents the threshold 10 mvolt.*

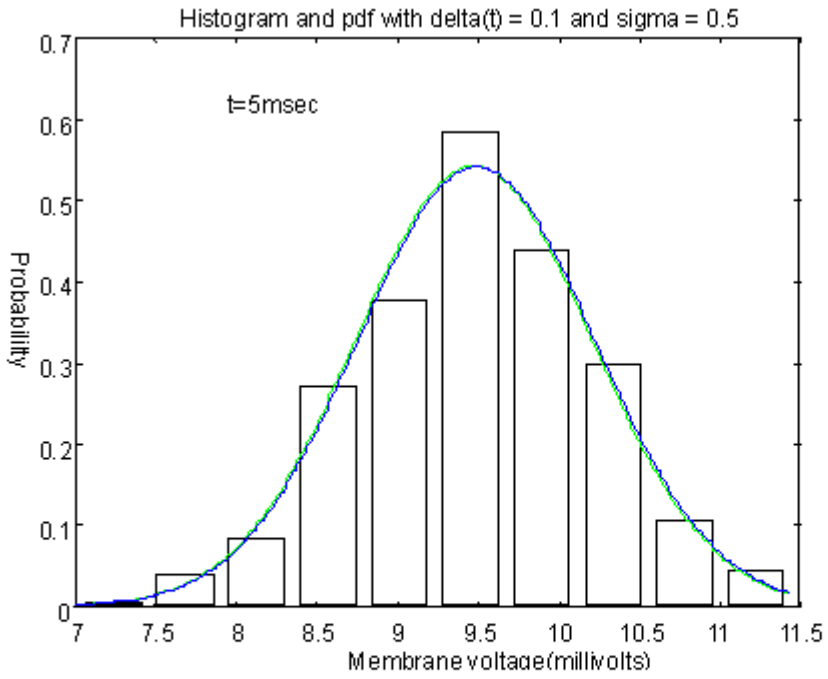

Figure 4.8. The histogram and pdfs of membrane voltage of the OU process at 5 *mesc. The total area of histogram bars is 1. The blue curve is pdf of the simulated membrane voltage, and the green curve is the pdf of expected membrane voltage at 5 mesc. The sample size of the random variable membrane is 400.*

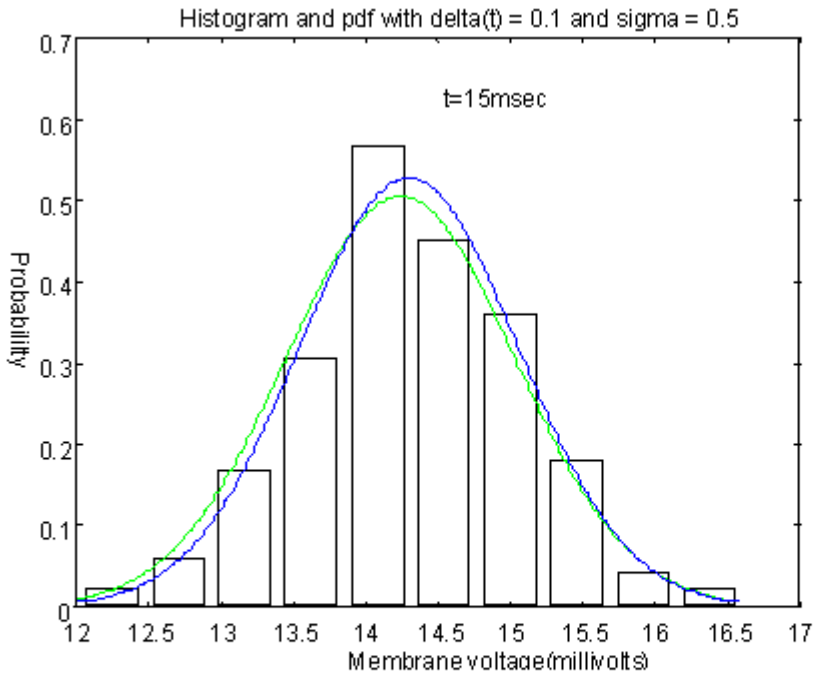

Figure 4.9. The histogram and pdfs of membrane voltage of the OU process at 15 *mesc. The total area of histogram bars is 1. The blue curve is pdf of the simulated membrane voltage, and the green curve is the pdf of expected membrane voltage at 5 mesc. The sample size of the membrane voltage is 400.*

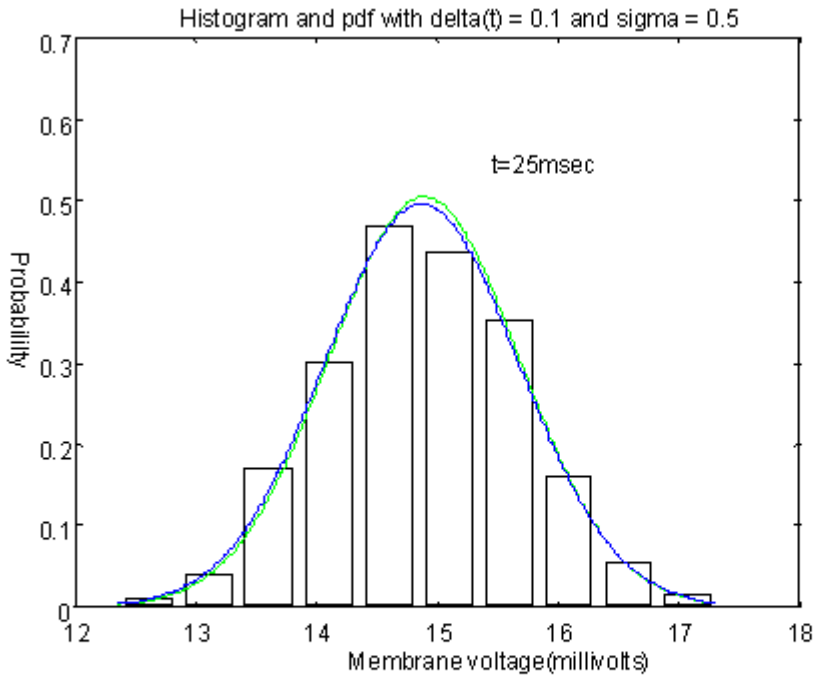

Figure 4.10. The histogram and pdfs of the membrane voltage of the OU process at 25 *mesc. The total area of histogram bars is 1. The blue curve is pdf of the simulated membrane voltage, and the green curve is the pdf of expected membrane voltage at 5 mesc. The sample size of the random variable membrane voltage is 400.*

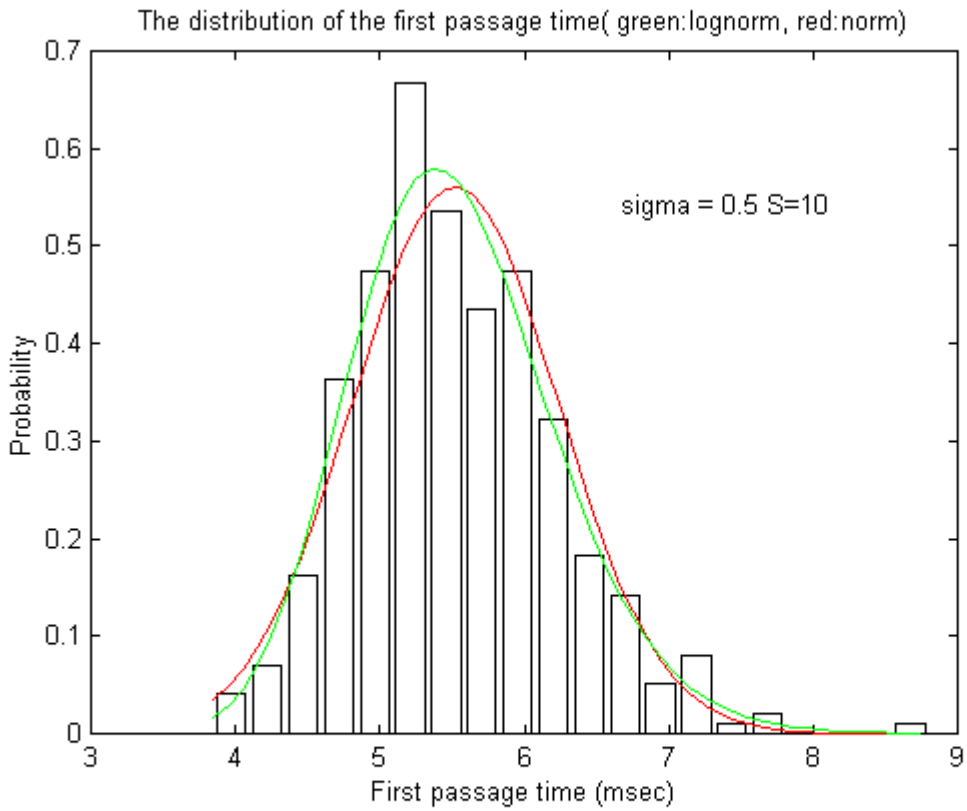

Figure 4.11. The histogram and the pdfs of FPT of the OU process with the Wiener process parameter 0.25 and the threshold 10 *mvolt*. *The green curve is fitted by lognormal density function and the red curve is fitted by normal density function.*

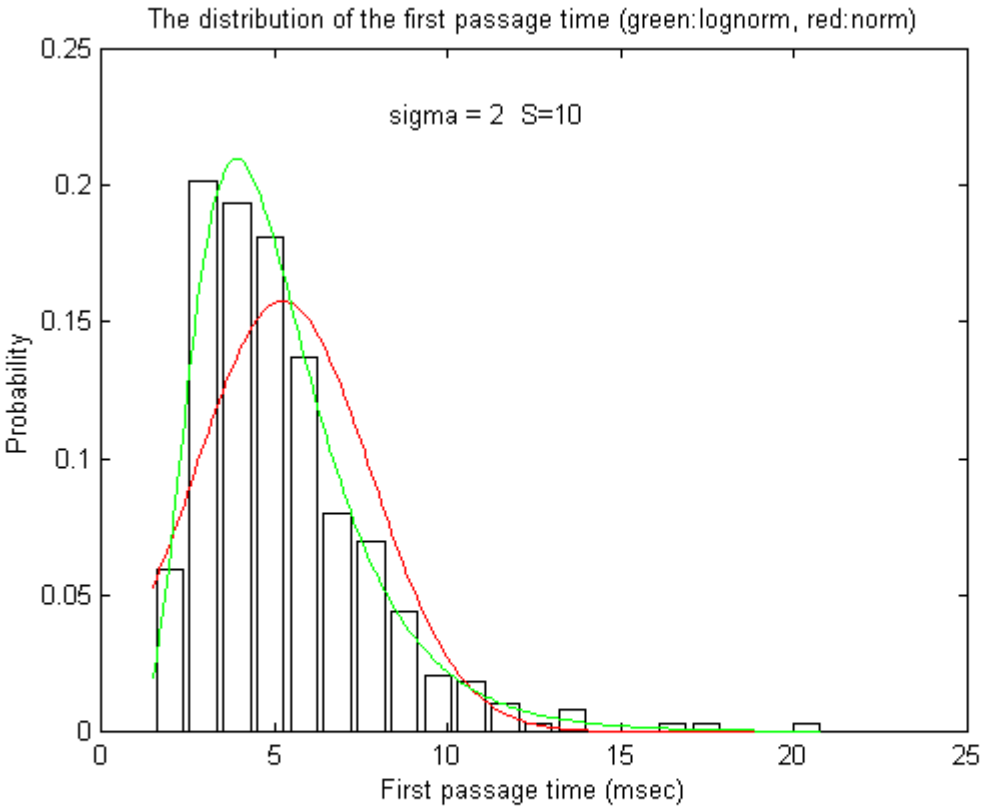

Figure 4.12. The histogram and the pdfs of FPT of the OU process with the Wiener process parameter 4 and the threshold 10 *mvolt*. *The green curve is fitted by lognormal density function and the red curve is fitted by normal density function.*

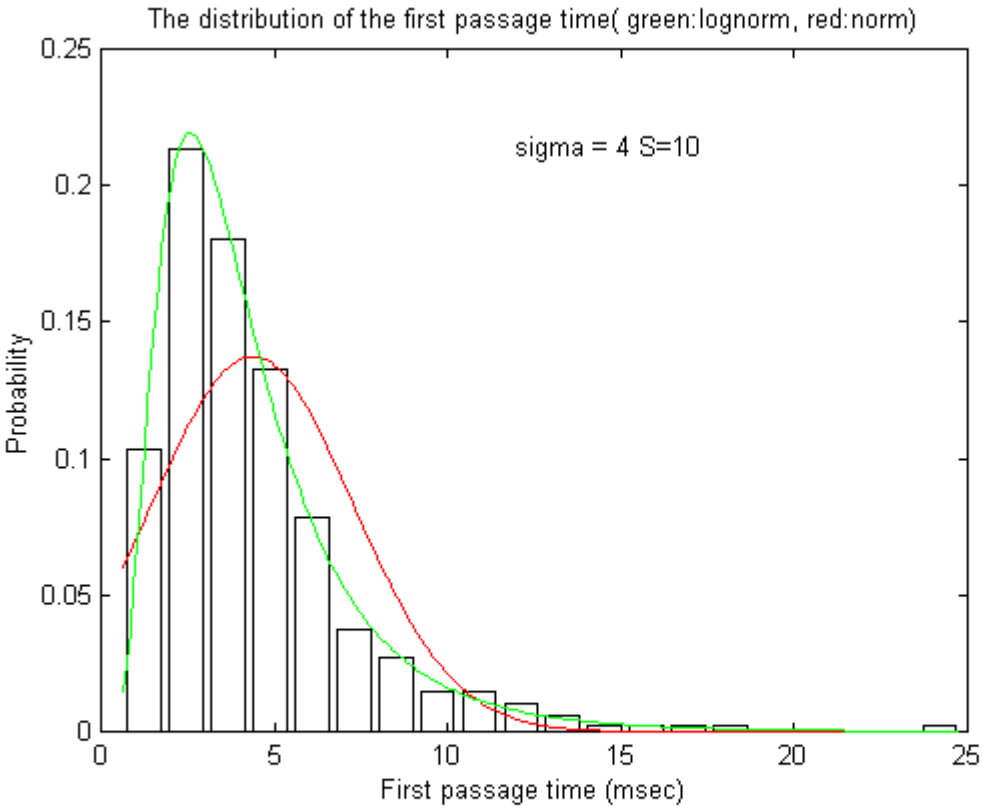

Figure 4.13: The histogram and the pdfs of FPT of the OU process with the Wiener process parameter 16 and the threshold 10 *mvolt*. *The green curve is fitted by lognormal density function and the red curve is fitted by normal density function.*

4.2 Approximation

1. **For the small Wiener process parameter, Stein's approximation values of the mean and variance of FPT are close to the simulated results.**

   When σ is 0.5, Figures 4.14 and 4.15 show that the mean and variance approximated using the Stein's method are very close to the simulated results. This is true except when the threshold is 14 *mvolt*. This tells us the approximation using Stein's method works well for a small Wiener parameter. For $\sigma = 2$, Figures 4.15 and 4.16 show that the approximated results deviate from the simulated results a lot, when the thresholds are greater than 9 *mvolt*. When σ is 4, Figures 4.18 and 4.19 show that the approximation results deviate from the simulated results very much, even if the threshold is very small. All the approximation results are out of the confidence interval (CI) of the simulated results. This result suggests that the Stein's method should not be used near the large Wiener parameter range in OU process.

2. **Using more terms of the Taylor's series, the approximation**

results are like Stein's method for the small Wiener parameter. But, this does not work well for a large Wiener process parameter.

When σ is 0.5, after adding the second term of the Taylor's series to Stein's method, approximation results are all very close to the simulation results. Figures 4.20 and 4.21 show this, except when threshold is greater than 12 *mvolt*.

When σ is 2, Figures 4.22 and 4.23 show that the approximation results still deviate from the simulation results a lot, for large thresholds. They also show that by using more terms, the deviations even occur for the small thresholds. Figures 4.24 and 4.25 tell us that for a large Wiener process parameter, σ is 2 or 4, the approximation does not work. All approximation results deviate from the simulation results a lot, particularly for large thresholds, such as 14 *mvolt*.

Because the third central moment of normal distribution is 0, the approximation results by using three terms are the same as those by two terms. Adding the higher order terms sometimes causes the variance to become negative. Hence, the third and higher order terms are not used.

3. **The approximation errors of two terms of the Taylor's series are less than those of one term, when σ is 0.5.**

The approximation errors are in Table 4.3 and Table 4.4. They show that the approximation errors for the mean and standard deviation of FPT by two terms of the Taylor's series are less than those by one term, when σ is 0.5. This is true except for the relatively small or relatively large threshold, such as the approximation error of the mean for threshold 12 *mvolt* and the approximation error of the standard deviation for threshold 6 *mvolt*. The approximation errors for the mean by four terms of the Taylor's series are very close to the approximation errors for the mean by two terms. But, the approximation errors for the standard deviation by four terms of the Taylor's series are greater than both those by one term and by two terms.

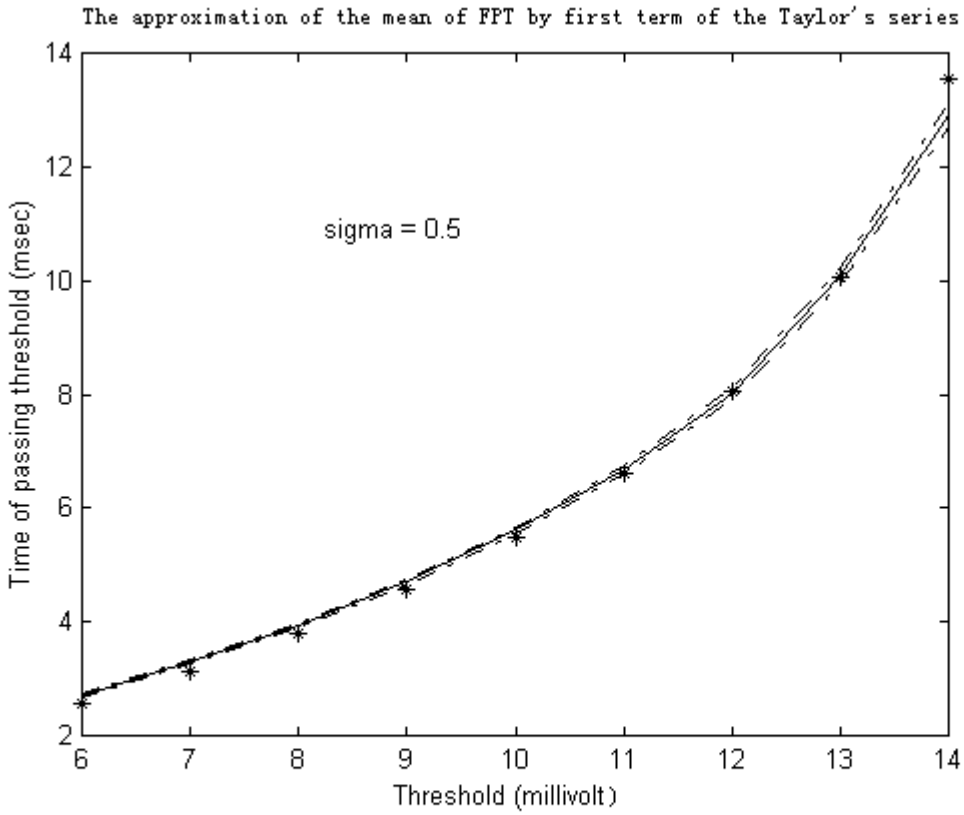

Figure 4.14. Stein's approximation for the mean of FPT by using the first term of the Taylor's series , where the Wiener process parameter is 0.25. *The central curve is the mean of membrane voltage from simulation and the other two curves beside it are the upper and lower 95% confidence limit for the mean FPT, respectively. "*" represents the approximation values by the first term of the Taylor's series.*

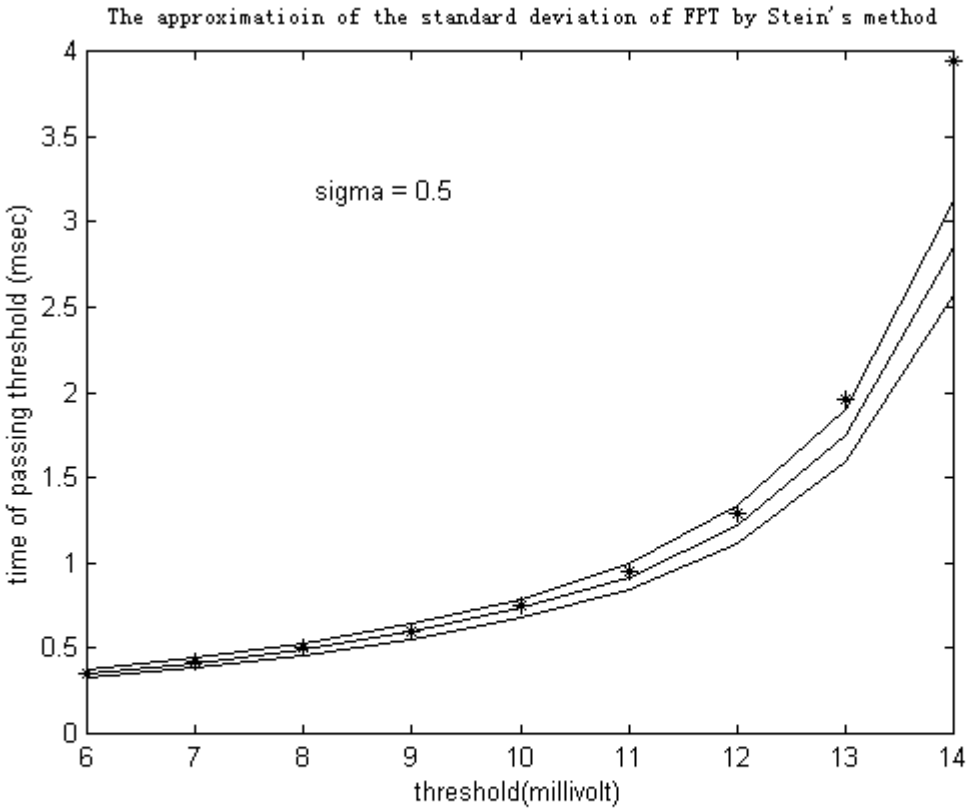

Figure 4.15. Stein's Approximation for the standard deviation of FPT by using the first term of the Taylor's series, where The Wiener process parameter is 0.25. *The central curve is the mean of membrane voltage from simulation and the other two curves beside it are the upper and lower 95% confidence limit respectively. "*" represents the approximated values by the first term of the Taylor's series.*

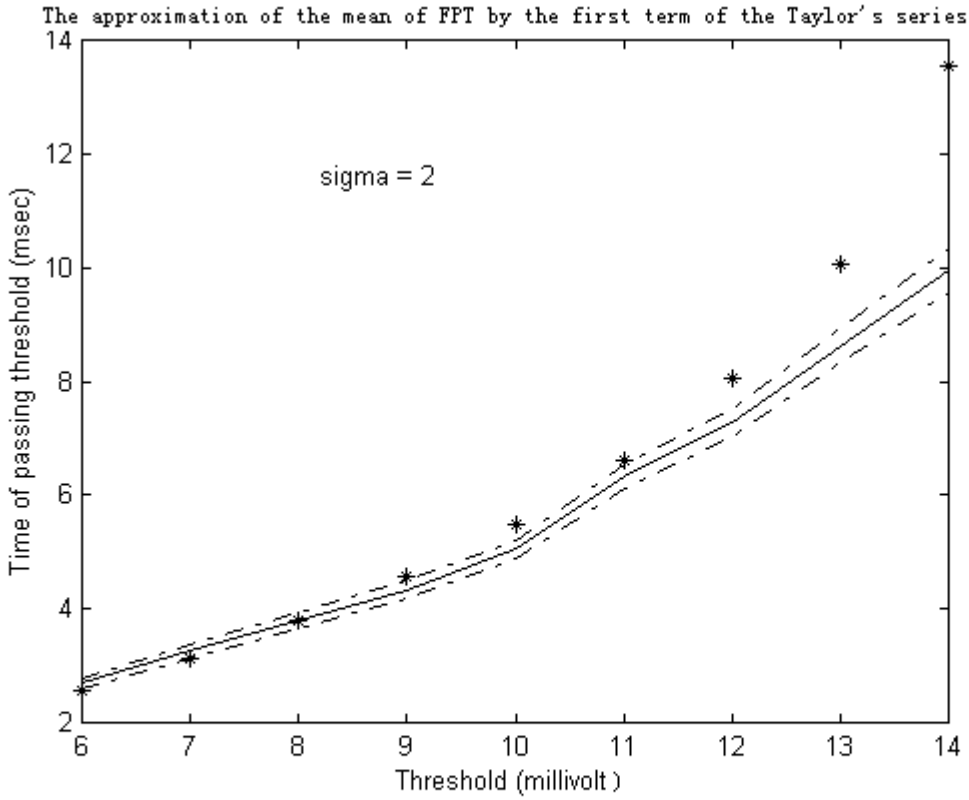

Figure 4.16. Stein's approximation for the mean of FPT by using the first term of the Taylor's series, where the Wiener process parameter is 4. *The central curve is the mean of membrane voltage from simulation and the other two curves beside it are the upper and lower 95% confidence limit for the mean FPT, respectively. "*" represents the approximated values by the first term of the Taylor's series.*

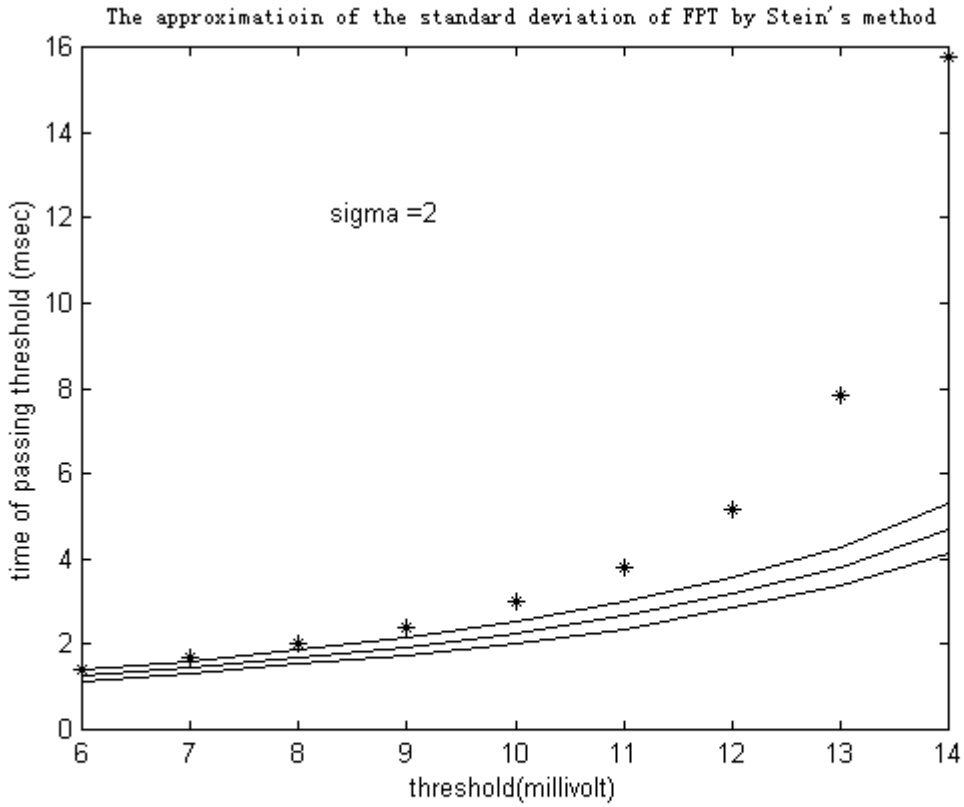

Figure 4.17. Stein's Approximation for the standard deviation of FPT by using the first term of the Taylor's series, where the Wiener process parameter is 4. *The central curve is the mean of membrane voltage from simulation and the other two curves beside it are the upper and lower 95% confidence limit respectively. "*" represents the approximated values by the first term of the Taylor's series.*

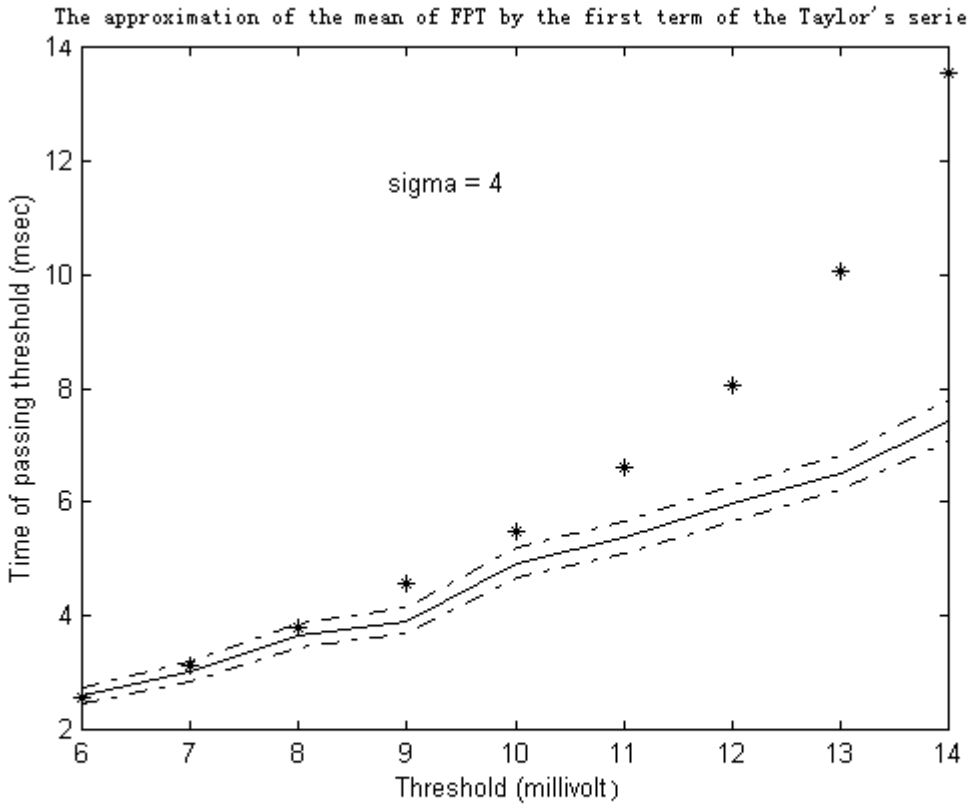

Figure 4.18. Stein's approximation for the mean of FPT by using first term of the Taylor's series, where the Wiener process parameter is 16. *The central curve is the mean of membrane voltage from simulation and the other two curves beside it are the upper and lower 95% confidence limit for the mean FPT, respectively. "*" represents the approximated values by the first term of the Taylor's series.*

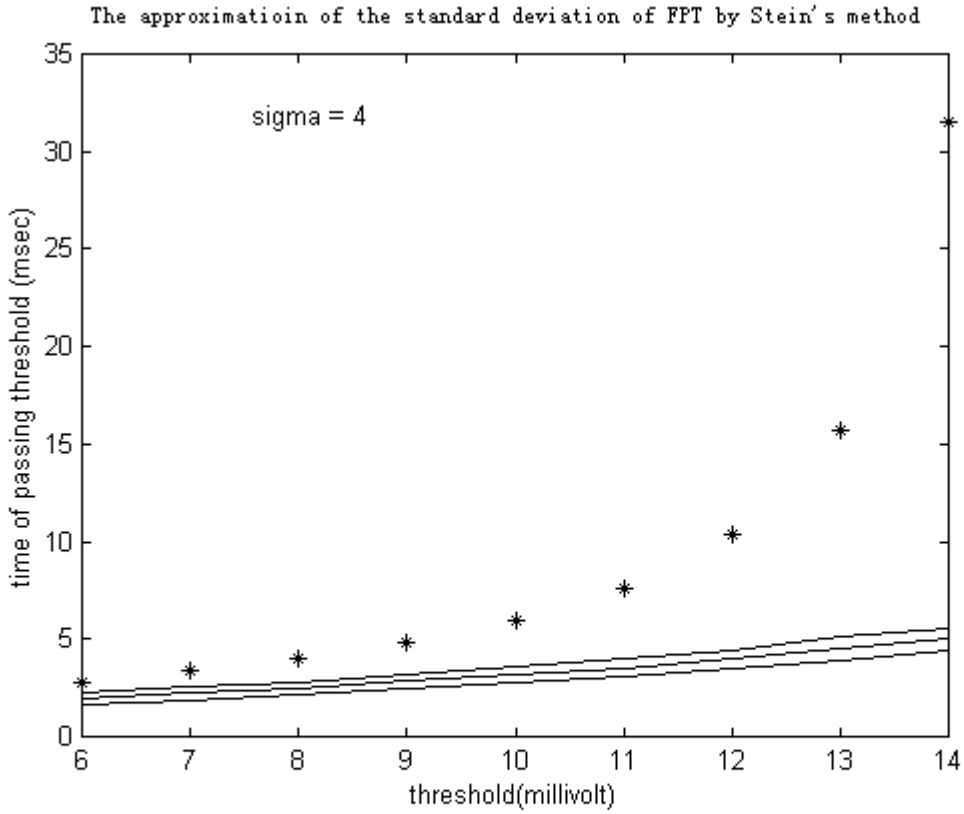

Figure 4.19. Stein's Approximation for the standard deviation of FPT by using the first term of the Taylor's series, where the Wiener process parameter is 16. *The central curve is the mean of membrane voltage from simulation and the other two curves beside it are the upper and lower 95% confidence limit respectively. "*" represents the approximated value by the first term of the Taylor's series.*

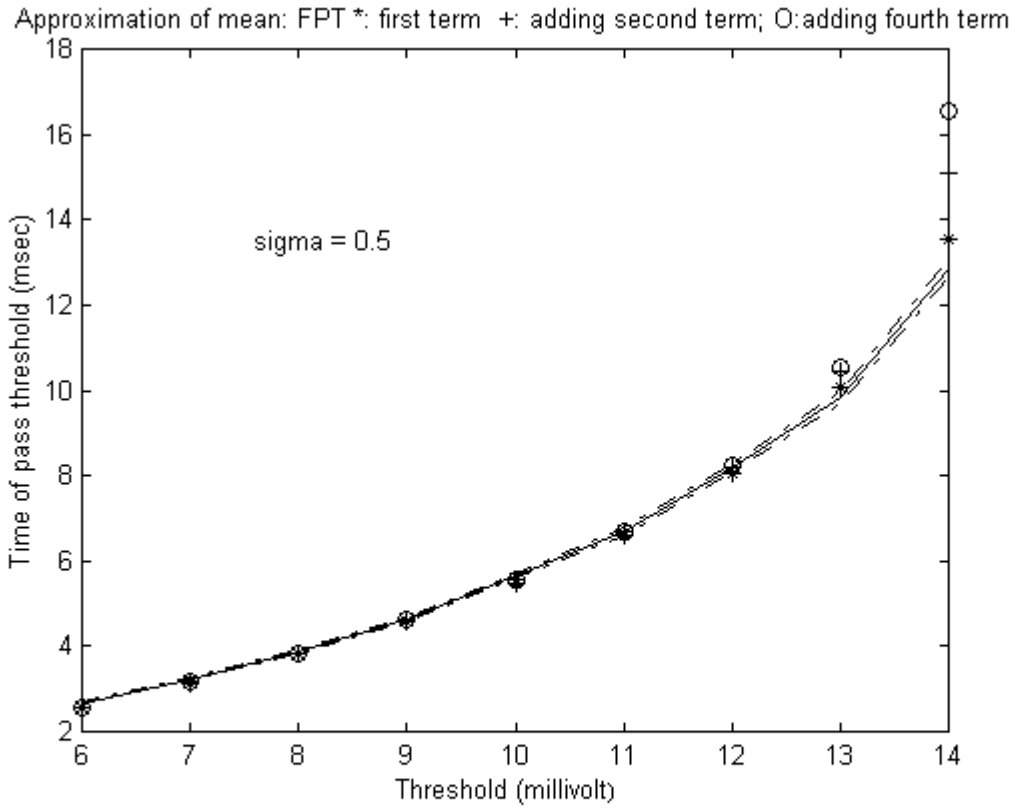

Figure 4.20. The Approximation for the mean of FPT by using two terms of the Taylor's series and four terms, where the Wiener process parameter is 0.25. *The central curve is the mean of membrane voltage from simulation and the other two curves beside it are the upper and lower 95% confidence limit, respectively. "*" represents the approximated values by the first term of the Taylor's series; "+" represents the approximated values by two terms; "∘" represents the approximated values by four terms.*

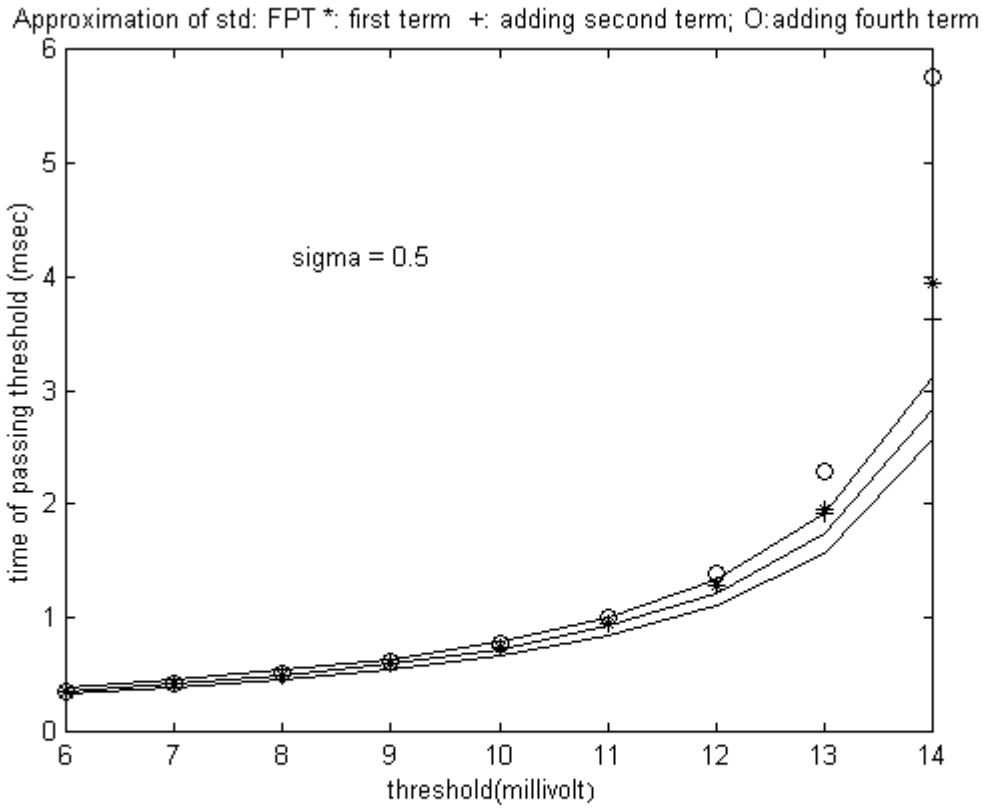

Figure 4.21. The Approximation for the standard deviation of FPT by using two terms of the Taylor's series and four terms, where the Wiener process parameter is 0.25. *The central curve is the standard deviation of membrane voltage from simulation and the other two curves beside it are the upper and lower 95% confidence limit, respectively. "*" represents the approximated values by the first term of the Taylor's series; "+" represents the approximated values by two terms; "∘" represents the approximated values by four terms.*

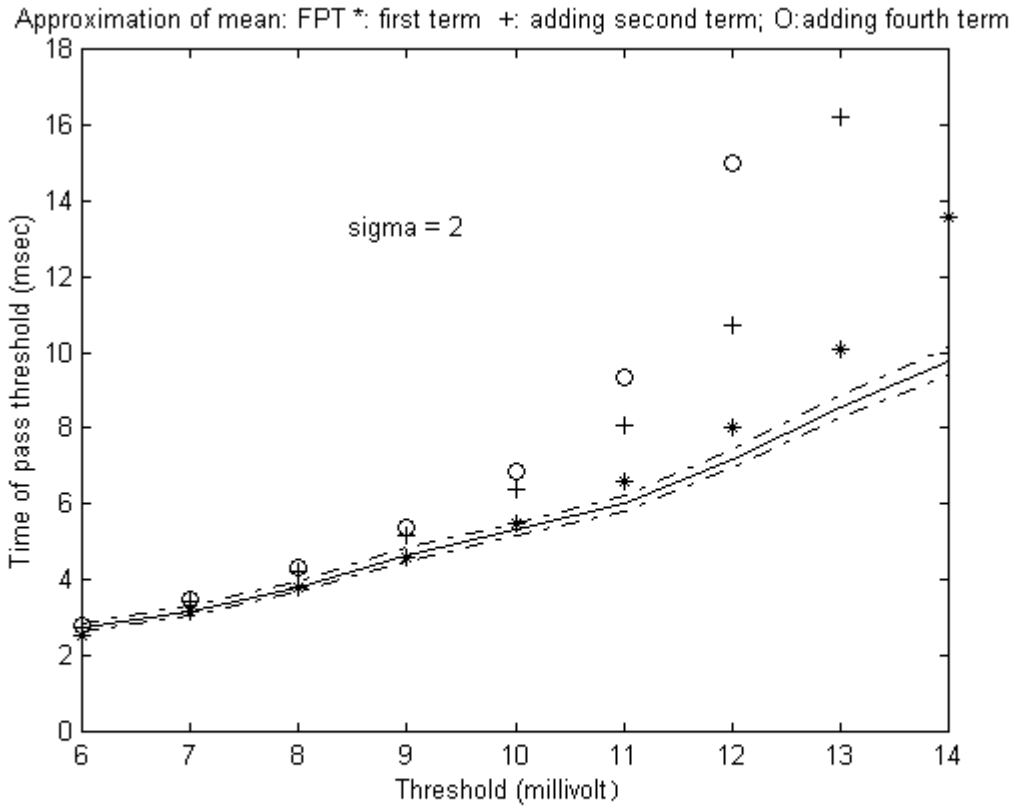

Figure 4.22. The Approximation for the mean of FPT by using two terms of the Taylor's series and four terms, where the Wiener process parameter is 4. *The central curve is the mean of membrane voltage from simulation and the other two curves beside it are the upper and lower 95% confidence limit, respectively. "*" represents the approximated values by the first term of the Taylor's series; "+" represents the approximated values by two terms; "∘" represents the approximated values by four terms.*

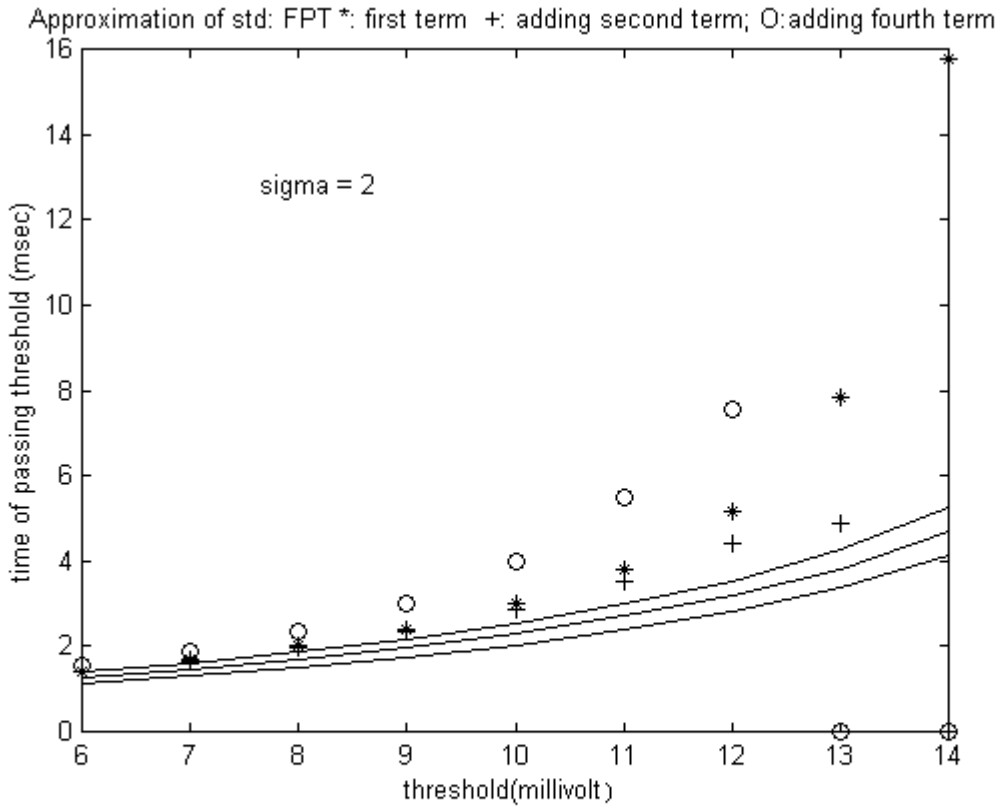

Figure 4.23. The Approximation for the standard deviation of FPT by using two terms of the Taylor's series and four terms, where the Wiener process parameter is 4. *The central curve is the standard deviation of membrane voltage from simulation and the other two curves beside it are the upper and lower 95% confidence limit, respectively. "*" represents the approximated values by the first term of the Taylor's series; "+" represents the approximated values by two terms; "∘" represents the approximated values by four terms.*

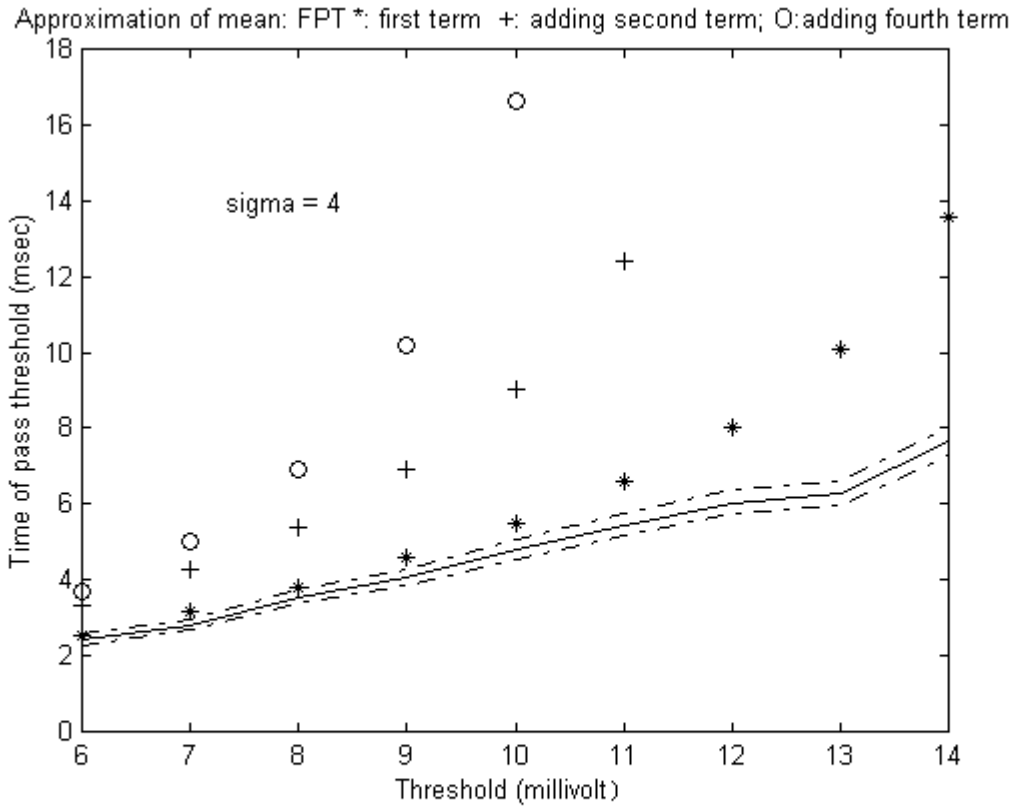

Figure 4.24. The Approximation for the mean of FPT by using two terms of the Taylor's series and four terms, where the Wiener process parameter is 16. *The central curve is the mean of membrane voltage from simulation and the other two curves beside it are the upper and lower 95% confidence limit, respectively. "*" represents the approximated values by the first term of the Taylor's series; "+" represents the approximated values by two terms; "∘" represents the approximated values by four terms.*

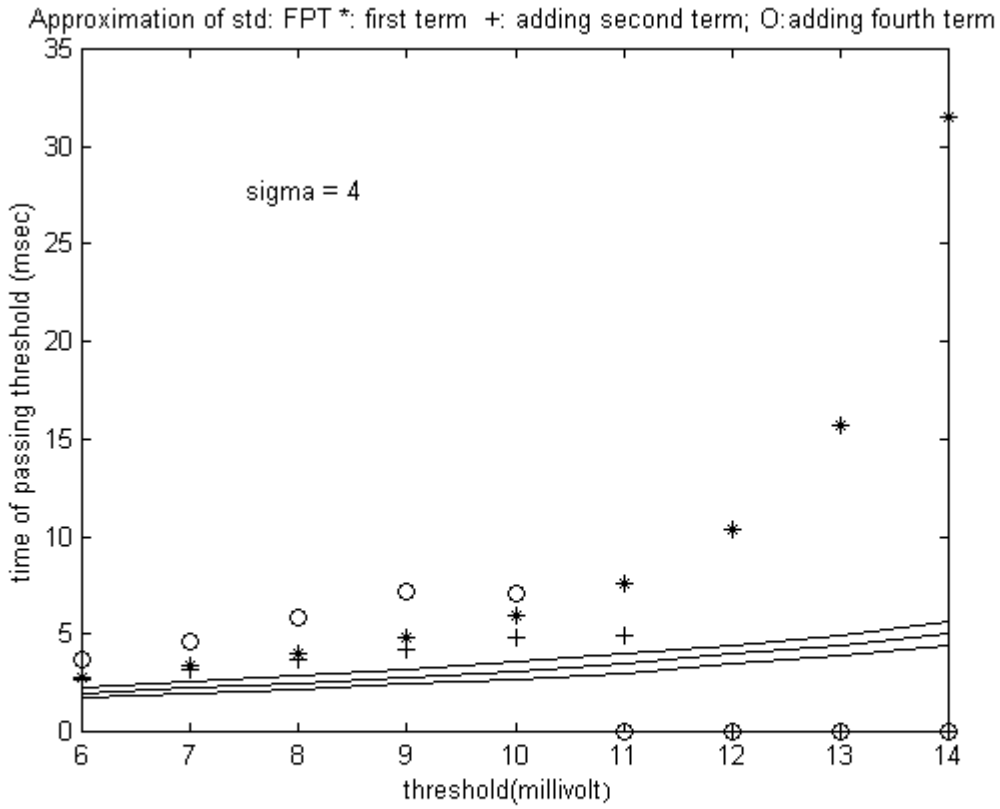

Figure 4.25. The Approximation for the standard deviation of FPT by using two terms of the Taylor's series and four terms, where the Wiener process parameter is 16. *The central curve is the standard deviation of membrane voltage from simulation and the other two curves beside it are the upper and lower 95% confidence limit, respectively. * represents the approximation value by first term of the Taylor's series; + represents the approximation value by two terms; o represents the approximation value by four terms.*

Table 4.3. The approximation errors of the mean of FPT by the different terms of the Taylor's series.

S(threshold)	one term		two terms		four terms	
mvolt	$error_{mean}$	std_{error}	$error_{mean}$	std_{error}	$error_{mean}$	std_{error}
6	-0.0528	0.0063	-0.0482	0.0063	-0.0482	0.0063
7	-0.0418	0.0063	-0.0364	0.0063	-0.0364	0.0063
8	-0.0335	0.0054	-0.0271	0.0055	-0.0270	0.0055
9	-0.0265	0.0055	-0.0187	0.0055	-0.0185	0.0055
10	-0.0202	0.0063	-0.0103	0.0063	-0.0100	0.0063
11	-0.0129	0.0080	0.0006	0.0081	-0.0014	0.0081
12	-0.0048	0.0074	0.0158	0.0076	0.0179	0.0076

$error_{mean}$ represents the approximation errors of the mean of FPT. std_{error} represents the standard deviation of the approximation errors. The sample size of approximation errors is 100. σ is 0.5.

Table 4.4. The approximation errors of the standard deviation of FPT by the different terms of the Taylor's series.

S(threshold)	one term		two terms		four terms	
mvolt	$error_{std}$	std_{error}	$error_{std}$	std_{error}	$error_{std}$	std_{error}
6	-0.0003	0.0338	-0.0010	0.0338	0.0058	0.0340
7	0.0057	0.0370	0.0048	0.0370	0.0144	0.0373
8	0.0009	0.0386	-0.0003	0.0386	0.0133	0.0391
9	0.0137	0.0338	0.0118	0.0388	0.0319	0.0395
10	0.0129	0.0390	0.0101	0.0389	0.0405	0.0401
11	0.0287	0.0403	0.0240	0.0401	0.0738	0.0420
12	0.0582	0.0457	0.0493	0.0453	0.1412	0.0493

$error_{std}$ represents the approximation errors of the standard deviation of FPT. std_{error} represents the standard deviation of the approximation errors. The sample size of approximation errors is 100. σ is 0.5.

4.3 Comparison of Two Probability Density Functions

We only compare density functions when the Wiener process parameter is small ($\sigma = 0.5$). This is done because the integral of the approximated pdf by Stein's method is less than 1, for the large Wiener process parameters. Figure 4.29 shows that the upper confidence limits of difference of Kullback–Leilber criteria are less than zero when the thresholds are from 6 *mvolt* to 9 *mvolt*, and at 13 *mvolt*. So, we reject null hypothesis and conclude Lognormal pdf is closer to the true pdf for thresholds from 6 *mvolt* to 9 *mvolt*, and at 13 *mvolt* (see Figures 4.26 and 4.28). In the median range of thresholds, from 10 *mvolt* to 12 *mvolt*, Figure 4.29 shows that the confidence intervals of difference of Kullback–Leilber criteria include zero (see Figure 4.27). Then, we do not reject null hypothesis and conclude that both pdfs are equally close to the true and unknown pdf of the FPT. But, we notice that when the null hypothesis is rejected, the upper limit of difference of Kullback–Leilber criteria is around 0.02, very close to zero. So, we can say that these two pdfs are almost equally close to the true and unknown pdf of the FPT when the Wiener parameter is 0.25 and thresholds are from 6 *mvolt* to 13 *mvolt*.

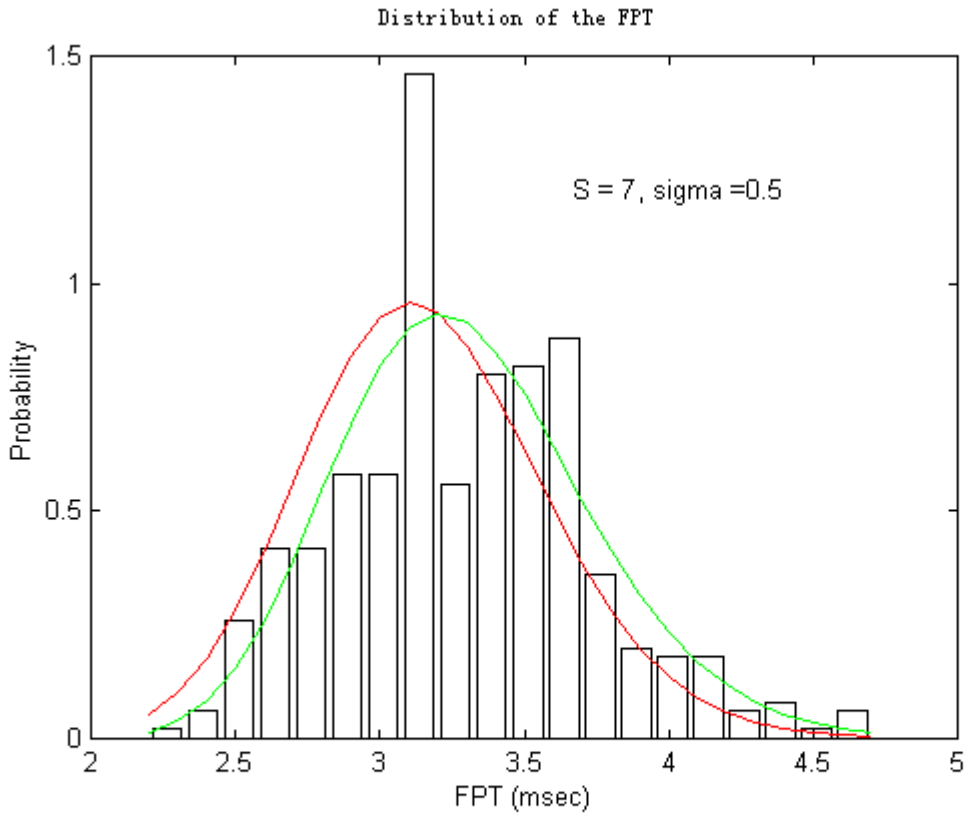

Figure 4.26. The histogram and pdfs of FPT with the threshold 7 *mvolt* and the Wiener process parameter 0.25. *The red curve is fitted by lognormal distribution and the green curve is approximated by Stein's method.*

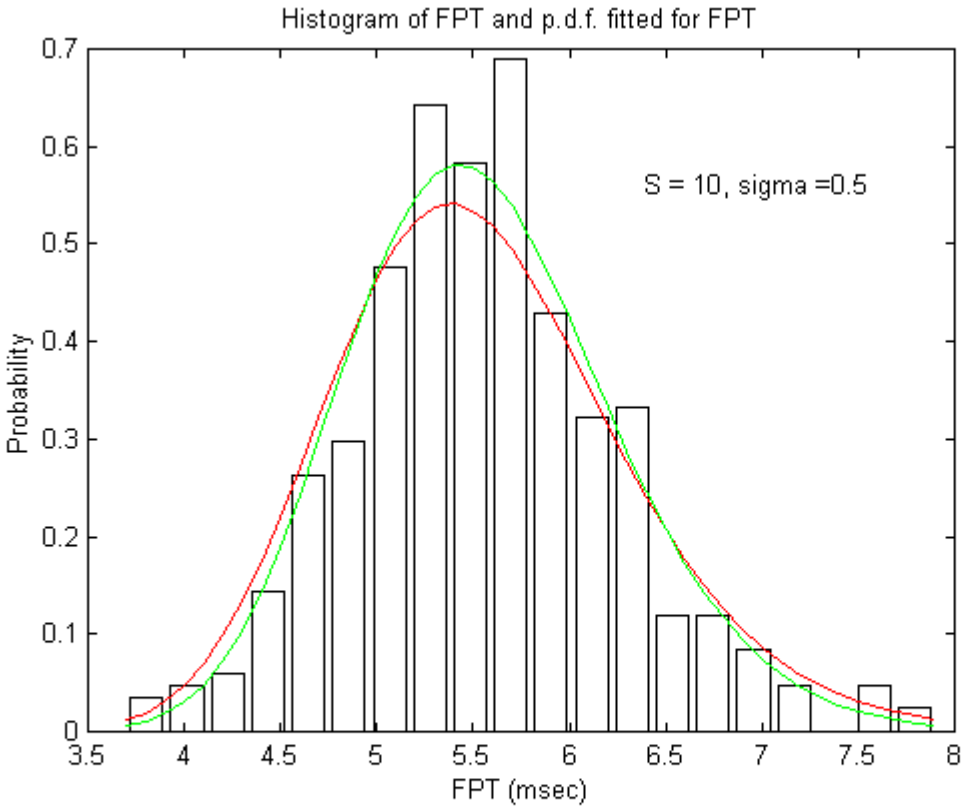

Figure 4.27. The histogram and pdfs of FPT with the threshold 10 *mvolt* and the Wiener process parameter 0.25. *The red curve is fitted by lognormal distribution and the green curve is approximated by Stein's method.*

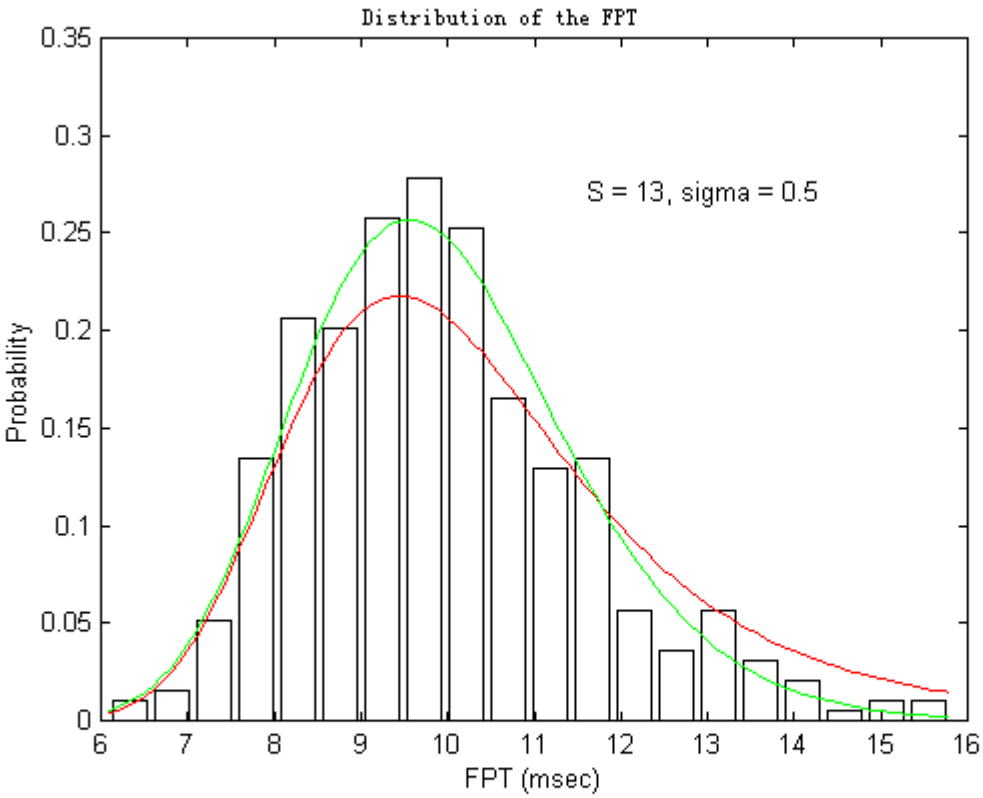

Figure 4.28. The histogram and pdfs of FPT with the threshold 13 *mvolt* and the Wiener process parameter 0.25. *The red curve is fitted by lognormal distribution and the green curve is approximated by Stein's method.*

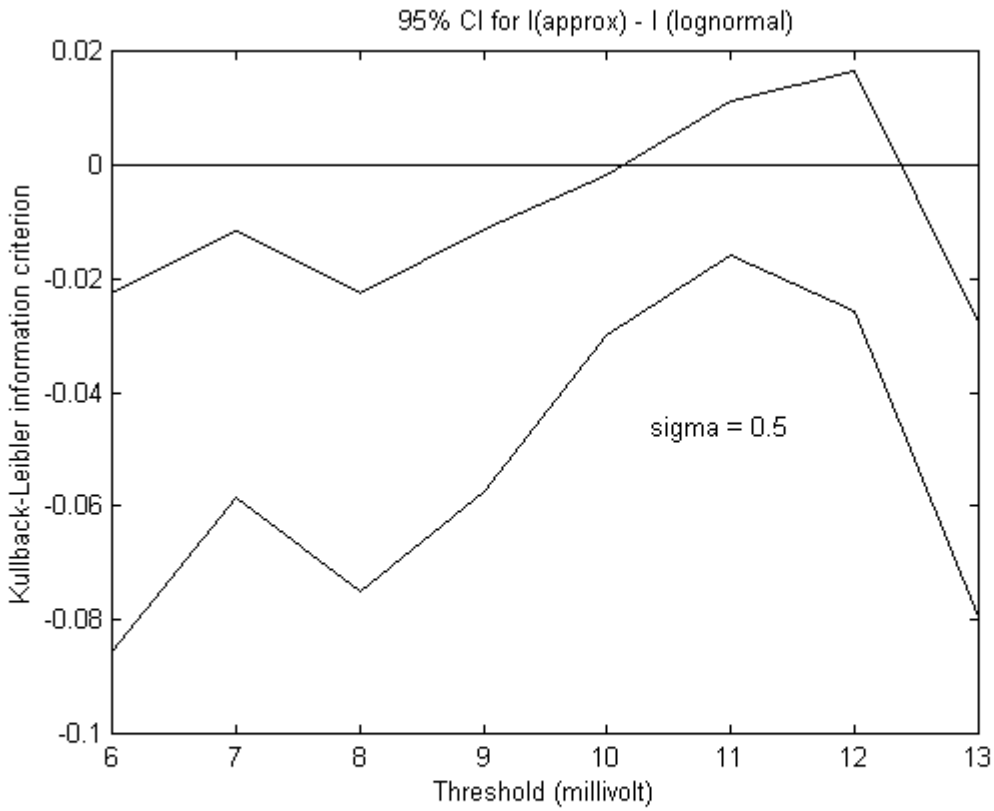

Figure 4.29. 95% confidence interval of the difference of Kullback–Leibler information criteria. *The two irregular curves are the 95% upper and lower limit for the difference of Kullback–Leibler information criteria of the approximated density functions of FPT and the fitted lognormal density functions.*

Chapter 5

Discussion

The use of the diffusion processes to model a neuron's membrane voltage has a long history. Interest in such models is still quite strong, as evidenced by recent work [22]. The most thorough studies about diffusions in this context are the Wiener and the OU processes. The latter arises as the continuous limit of Stein's model and plays a central role because it naturally arises when starting from an equivalent electric circuit of the membrane potential of real neurons at subthreshold level. The Wiener Process yields the inverse Gaussian distribution for the FPT, which is analytically tractable, so that standard inferential procedures (parameter estimation, confidence intervals, goodness of fit tests) have been well developed. That is not the case for the

OU process or other models. This paucity of statistical methods for biologically more realistic models has led to the use of rather ad hoc procedures, such as the use of moments or curve fitting using generic distributions for positive random variables, such as lognormal. Recent work [11] has alleviated some of these difficulties, but much still remains to be done.

Using Stein's method to approximate the FPT of the OU process, The approximation values of the FPT we obtain are the time at which $E(x(t))$ reaches S, shown as t^* in Equation (2.12) and in Figure 2.3. The smaller the variance of $x(t)$, the better we expect this approximation will to be, since it is exact in the limiting case of zero variability. The variance of $x(t)$ is $Var[x(t)] = \sigma^2\tau(1 - e^{-\frac{2t}{\tau}})/2$, in which τ is a constant and t is around t^*. So, the variance of $x(t)$ is only dependent on the Wiener process parameter. When σ is small, the variance of $x(t)$ will be smaller. So, we expect that when σ is small, this approximation will be better. This is consistent with our result that when σ is 0.5, the approximation works very well. Another reason that the approximation by Stein's method can work in the OU process may be related to the fact that the OU process has a relatively long correlation time which is one condition for Stein's method to work.

When σ is large, such as 2 or 4, the approximated results deviate from

the simulated FPT very much, depending on the thresholds. This result is not surprising because when σ is large, its higher order power in the Taylor's series will dominate the approximation results.

Since the original Stein's method can approximate the FPT of the OU process, this approach results in the possibility to consider not only the Stein's approximation method, but also some of its generalizations and modifications. When the Wiener parameter, σ^2, is 0.25, the approximation errors of the mean and standard deviation for two terms of the Taylor's series are less than those for one term. It appears that the terms with higher order power of the Wiener parameter, such as second power and fourth power, are large enough to keep to obtain more precise results, when σ is 0.5. So, depending on the Wiener parameter, using more terms of the Taylor's series sometimes can help to obtain better approximation.

Our results give in depth evidence that lognormal density function is close to the true distribution of the FPT. For the other FPT histogram, exponential and gamma densities provide good fits in the numerous reports and for certain limiting parameter values. This suggests that these simple densities can approximate the OU process. S. Iyengar and Q. Liao (1997) reported that inverse Guassian distribution is closer to the true pdf than lognormal

distribution when they approximated the OU process. But, the inverse Guassian has three parameters to estimate. It is reasonable that three parameter distribution fits better to the data than two parameter distribution does.

The approximation of the FPT of the OU process is the only purpose of this article and we do not intend to present here a mathematical analysis of the OU process. Namely, the formal description of neuronal firing in the terms of the first passage time problem remains untouched. One disadvantage of this article is that there is no real data to check the approximation results. We hope to investigate both of them in our later work.

Chapter 6

Conclusions

1. When σ is 0.5, the approximation results of Stein's method are in the confidence interval of the mean and variance of FPT. So, we can say that Stein's method works well for the OU process with a small Wiener process parameter.

2. When σ is 2 or 4, using more terms of the Taylor's series is not seen to improve the approximation of the mean and variance of the first passage time for the OU process.

3. When σ is 0.5, the approximation errors for the approximation with first two terms of the Taylor's series are smaller than the approximation with first term dose. This suggests that in the range within which the

approximation of Stein's method works well, we can get more precise approximation by using the first two terms of the Taylor's series.

4. Lognormal pdf fitted for simulation data is close to the true distribution of the FPT of the OU process for all the Wiener process parameter we use.

Bibliography

[1] G. Bugmann, 1991. *Summation and Multiplication: Two Distinct Operation Domains of Leaky Integrate–and–fire Neurons*. Network 2: 489–509.

[2] R. M. Capocelli and L. M. Ricciardi, 1971. *Diffusion Approximation and First Passage Time Problem for a Model Neuron*. Kybernetik 8: 214–223.

[3] G. Cerbone, L. M. Ricciardi and L. Sacerdote, 1981. *Mean Variance and Skewness of the First Passage Time for the Ornstein–Uhlenbeck Process*. Cybern. Syst. 12: 395–429.

[4] J. L. Devore, 2000. *Probability and Statistics for Engineering and the Sciences*. Duxbury 5th ed. Pacific Grove. pp265–273.

[5] C. H. Edwards and D. E. Penney, 2000. *Elementary Differential Equations With Boundary Value Problems*. 4th ed. Prentice–Hall, New Jersy.

pp436–437.

[6] R. V. Foutz, and R. C. Srivastava, 1977. *The Performance of the Likelihood Ratio Test When the Model is Incorrect*. Ann. Statist. 5: 1183-1194.

[7] R. O. Gilbert, 1987. *Statistical Methods for Environmental Pollution Monitoring*. Van Nostrand Reinhold, New York. pp165–175.

[8] V. Giorno, P. Lánský, A. G. Nobile and L. M. Ricciardi, 1988. *Diffusion Approximation and First Passage Time Problem for a Model Neuron*. Biol. Cybern. 58: 387–404.

[9] D. Hansel, G. Mato, C. Meunier and L. Neltner, 1998. *On Numerical Simulations of Integrate–and–Fire Neural Networks*. Neural Comput. 10: 467–483.

[10] A. V. Holden, 1976. *Models of the Stochastic Activity of Neurons*. Springer–Verlag, New York.

[11] J. Inoue, S. Sato and L. M. Ricciardi, 1995. *On the Parameter Estimation for Diffusion Models of Single Neuron's Activities*. Biol. Cybern. 73: 209–221.

[12] S. Iyengar and Q. Liao, 1997. *Modeling Neural Activity Using the Generalized Inverse Gaussian Distirbution*. Biol. Cybern. 77: 289–295.

[13] D. H. Johnson, 1996. *Point Process Models of Single–Neuron Discharges*. J. Comput. Neurosci. 3: 275–299.

[14] E. R. Kandel and J. H. Schwartz, 1985. *Principles of Neural Science*. 2ed Edition. Elsvier, New York. pp75–86.

[15] P. E. Kloeden, E. Platen and H. Schurz, 1994. *Numerical Solution of SDE Through Computer Experiments*. Springer–Verlag, New York. pp110–111.

[16] P. Lánský, 1984. *On Approximations of Stein's Neuronal Model*. J. Theor. Biol. 107: 631–647.

[17] P. Lánský and V. Lánská, 1987. *Diffusion Approximation of the Neuronal Model with Synaptic Reversal Potentials*. Biol. Cybern. 56: 19–26.

[18] P. Lánský and C. E. Smith, 1989. *The Effect of a Random Initial Value in Neural First–Passage–Time Models*. Mathematical Bioscience 93: 191–215.

[19] P. Lánský, C. E. Smith and L. M. Ricciardi, 1990. *One–Dimensional Stochastic Diffution Models of Neuronal Activity and Related First Passage Time Problems*. Trends in Biological Cybernetics 1: 153–162.

[20] P. Lánský and M. Musila, 1991. *Variable Initial Depolarization in Stein's Neuronal Model with Synaptic Resversal Potentials*. Biol. Cybern. 64: 285–291.

[21] P. Lánský, M. Musila and C. E. Smith, 1992. *Effects of Afterhyperpolarication on Neuronal Firing*. BioSystems. 27: 25–38.

[22] P. Lánský, and J. P. Pospars, 1995. *Ornstein–Uhlenbeck Model Neuron Revistied*. Biol. Cybern. 72: 397-406.

[23] P. Lánský and R. Rodriguez, 1999. *The Spatial Properties of a Model Neuron Increase its Coding Range*. Biol. Cybern. 422: 0050–7.

[24] P. Lánský and R. Rodriguez, 1999. *Two–compartment Stochastic Model of a Neuron*. Physica D. 132: 267–286.

[25] P. Lánský and S. Sato, 1999. *The Stochastic Diffusion Models of Nerve Membrane Depolarization and Interspike Interval Generation*. J. Peripher. Nerv. Syst. 4(1): 27-42.

[26] L. Lapin, 1997. *Modern Engineering Statistics*. Duxbury, Belmont. pp318–319.

[27] M. Musial and P. Lánský, 1991. *Generalized Stein's Model for Anatomically Complex Neurons*. Biol. System. 25: 179–191.

[28] R. Nishii, 1988. *Maximum Likelihood Principle and Model Selection When the True Model is Unsepecified.* In: Rao C. R., Rao M. M. (des) Multivariate Statistics and Probability. Academic Press, New York, pp392–403.

[29] A. Papoulis, 1965. *Probability, Random Variables, and Stochastic Processes*. Mcgraw–Hill, New York. pp116-152.

[30] H. E. Plesser and S. Tanaka, 1997. *Stochastic Resonance in a Model Neuron With Reset*. Physics Letters A 225: 228–234.

[31] L. M. Ricciardi, 1976. *Diffusion Approximation for a Multi–Input Model Neuron*. Biol. Cybern. 24: 237–240.

[32] L. M. Ricciardi and L. Sacerdote, 1979. *The Orstein–Uhlenbeck Process as a Model for Neuronal Activity*. Biol. Cybernetics 35: 1–9.

[33] L. M. Ricciardi, L. Sacerdote and S. Sato, 1984. *On an Integral Equation for First–Passage–Time Probability Densities*. J. Appl. Prob. 21: 302–314.

[34] G. Sampath and S. K. Srinivasan, 1977. *Stochastic Models for Spike Trains of Single Neurons*. Springer–Verlag, New York.

[35] C. E. Smith and M. V. Smith, 1984. *Moments of Voltage Trajectories for Stein's Model with Synaptic Reversal Potentials*. J. Theoret. Neurobiolol. 3: 67-77.

[36] C. E. Smith, 1992. *A Heuristic Approach to Stochastic Models of Single Neurons*. "Single Neuron Computation", Academic Press, pp561–588. ISBN 0–12–48485–X.

[37] C. E. Smith, 1992. *A Note on Neuronal Firing and Input Variability* . J. Theor. Biol. 154: 271–275.

[38] R. B. Stein, 1965. *A Theoretical Analysis of Neuronal Variability*. Biophy. J. 5: 180–191.

[39] D, Tal and E. L. Schwartz, 1997. *Computing with the Leaky Intergrate–and–Fire Neuron: Logarithmic Computation and Multiplication*. Neural Comput. 9: 305–318.

[40] G. B. Thomas, 1972. *Calculus and Analytic Geometry* Assison–Wesley, New York. pp62–112.

[41] H. C. Tuckwell and W. Richter, 1978. *Neuronal Interspike Time Distributions and the Estimation of Neurophysiological and Neuroanantomical Parameters*. J. Theor. Biol. 71: 167–183.

[42] H. C. Tuckwell and D. K. Cope, 1980. *Accuracy of Neuronal Interspike Times Calculated from a Diffusion Approximation*. J. Theor. Biol. 83: 377–387.

[43] H. C. Tuckwell, 1988. *Introduction to Theoretical Neurobiology: Volume2 Nonlinearand Stochastic Theories*. Cambridge University Press, New York. pp150–168.

[44] H. C. Tuckwell, 1995. *Elementary Applications of Probability Theory*. Chapman and Hall, New York. 2nd ed. pp92–95.

[45] H. White, 1982. *Maximum likelihood Estimation of Misspecified Models.* Econmetrica 50(1): 1-26.

[46] W. J. Wilbur and J. Rinzel, 1982. *An Analysis of Stein's Model for Stochastic Neuronal Excitatioin.* Biol. Cybern. 45: 107–114.

Appendix A

Matlab Program

```
clear;

% The first passage time.

X0 = 0;                 % initial value of x(t).

DELTA_T = 0.1;                  % msec, interval of time, i. e. variance.

SIGMA = 0.5;                % Wiener parameter, SIGMA^2

TAU = 5;                % msec, membrane constant

SIZE = 1000;

MU = 3;                 %mv/msec, mean of input

MEAN = 0;

t = 0: DELTA_T:(SIZE*DELTA_T) ;                 % generate SIZE of t
```

```
Ex(1,1) = X0;                % initial value of x
Run_times = 400;             % the sample size of FPT
for THRESHOLD = 6:14;        % mvolt
   for J = 1:Run_times
   % standard normally distributed random numbers
      N = randn([1,SIZE]);
      n = MEAN + SIGMA*N*sqrt(DELTA_T);
      x(J,1) = X0;
      for I = 1: SIZE
            x(J,I+1) = x(J,I) + (MU - x(J,I)/TAU)*DELTA_T + n(1,I);
            if x(J,I)< THRESHOLD & x(J,I+1)>= THRESHOLD
            % the first passage condition
                  y(THRESHOLD-5,J) = (I+1)*DELTA_T;
                  %first passage time
                  break;              %guarantee the first passage
            end
      end
   end
end
```